Journal of Vibration Engineering & Technologies
https://doi.org/10.1007/s42417-024-01447-4

ORIGINAL PAPER

Effects of Operational and Environmental Conditions on Estimated Dynamic Characteristics of a Large In-service Wind Turbine

Onur Ozturkoglu[1] · **Ozgur Ozcelik**[1] · **Serkan Günel**[2]

Received: 3 April 2024 / Revised: 22 May 2024 / Accepted: 23 May 2024

Abstract

Purpose The reliable and continuous operation of wind turbines is of utmost importance, making it necessary to thoroughly understand their dynamic behavior under various operational and environmental conditions.

Methods To achieve this, a data acquisition system distributed throughout the tower height is designed. The system records data such as the acceleration, temperature, and relative humidity from the sensors, along with the rotor speed, wind speed, temperature, pitch angle, nacelle direction, and wind direction from the data acquisition system of the turbine. The acquired data is synchronized and processed by Autonomous and Continuous System Identification system based on the poly-reference Least Squares Complex Frequency method. The extensive dataset, gathered over a 7-month period, allows for the estimation of modal parameters of the wind turbine. The modal parameters are then correlated with the operational and environmental conditions that were recorded. The relationships between these conditions are thoroughly analyzed and explained. Additionally, the operational principles of the wind turbine are elucidated in detail. The correlations between the modal parameters and operational or environmental factors are presented and interpreted, shedding light on the complex interplay between wind turbine dynamics and external conditions.

Conclusion It can be said that changes in operational and environmental conditions affect the modal parameters of the wind turbine differently across various structural modes. Without considering these effects, structural health monitoring systems may produce false alarms. Failure to consider these effects in the development of structural health monitoring systems may lead to incorrect damage alarms.

Keywords Wind turbine · Operational and environmental conditions · Automated system identification · Data acquisition · Field testing

Introduction

Over the past few decades, wind energy has emerged as a prominent renewable energy option, offering advantages such as higher capacity utilization rates and quicker returns on investments compared to conventional energy generation methods. The global wind energy market has experienced remarkable growth over the last decade. Projections indicate that this growth trend will continue, with wind energy capacity estimated to surge to 3105.9 GW by 2030, representing an astounding increase of 374% [1]. This expansion in the wind energy sector is driving significant investments in the development of taller, larger, and more advanced wind turbines, even in regions prone to high seismic activity. In order to ensure the continuous generation of energy and the sustained operational efficiency of wind turbines throughout their operational lifespan, there is a growing need to monitor the structural integrity of these expansive structures and attain a comprehensive understanding of their structural dynamics, particularly under varying operational and environmental conditions [2–4]. One significant challenge associated with characterizing the dynamic behavior of wind turbines in operation lies in addressing the time-varying nature of the system. This variation arises from a multitude of factors, including the presence of rotating components such as rotor blades and the turbine nacelle, wind speed, blade pitch angle, wind direction, temperature, and relative humidity.

✉ Onur Ozturkoglu
onur.ozturkoglu@deu.edu.tr

[1] Department of Civil Engineering, Dokuz Eylul University, 35160 Izmir, Turkey

[2] Department of Electrical and Electronics Engineering, Dokuz Eylul University, 35160 Izmir, Turkey

Published online: 10 June 2024

Conducting field tests on full-scale structures plays a pivotal role in ascertaining the dynamic characteristics of these structures under realistic operational and environmental conditions. Operational Modal Analysis (OMA), also referred to as output-only modal analysis, revolves around measuring a structure's response (output) while leveraging the ambient and inherent operational vibrations as unmeasured inputs for system identification. Unlike modal identification methods that rely on input–output data, OMA techniques can be applied in real operating scenarios and situations where externally stimulating the structure may be challenging or unfeasible. OMA methods are aptly employed for assessing structures in their actual operating state, providing estimates of operational natural frequencies, damping ratios, and mode shapes that inherently differ from those obtained under non-operational circumstances [5, 6]. In operational modal analysis, a foundational assumption rests upon the time-invariant nature of the monitored structure. However, this assumption encounters some challenges due to the presence of moving or rotating components and the influence of environmental conditions. An advanced frequency domain estimation technique known as 'poly-reference Least Square Complex Frequency' (p-LSCF) has been introduced to address the issue [7–9]. This non-iterative method operates within the frequency domain and enables highly accurate system modal parameter estimation. Notably, the p-LSCF method offers cleaner stabilization diagrams than other modal parameter estimation approaches. In the context of this study, which aims to establish an autonomous system identification system without any user intervention, clean stabilization diagrams hold significant importance. These diagrams allow the system to determine the peak points precisely, thereby accurately extracting the physical mode frequencies. Employing this technique facilitates the extraction of modal parameters from an operational structure, such as a wind turbine, without interrupting its operation. This capability is essential in the case of wind turbine systems, as shutting them down would result in economic losses. Furthermore, when the system is deactivated, it enters a different dynamic state with identified characteristics distinct from those during operational conditions. Hence, characterizing a wind turbine under normal operating conditions holds particular significance.

Numerous studies have contributed to the field of wind turbine dynamics and health monitoring. James, Carne, and Lauffer [10] introduced the Natural Excitation Technique (NExT) for operational modal analysis, a widely used method for estimating modal parameters in the ambient environment. Häckell and Rolfes [11] developed a triangulation-based approach to extract modal parameters from a 5 MW wind turbine. At the same time Kilic and Unluturk [12] presented the Supervised Event Server Health Monitoring System (SESHMS) for cost-effective data acquisition and wind turbine performance estimation. Alves et al. [13] introduced Delphos, an instantaneous damage detection system for wind turbine blades, and Avendaño-Valencia and Fassois [14] employed a Gaussian Mixture Model Random Coefficient (GMM-RC) model-based method for robust damage diagnosis in an offshore 5 MW wind turbine. García & Tcherniak [15] demonstrated single-accelerometer-based monitoring of large turbine blades using a data-driven vibration structural health monitoring method. Kim, Kim, and Choe [16] investigated structural health monitoring for floating offshore wind turbines, highlighting the efficacy of curvature mode shapes in damage detection. Zhou et al. [17] explored the dynamic characteristics of monopile offshore wind turbines, emphasizing the applicability of the eigensystem realization algorithm method and wake mode identification. Zhao & Lang [18] introduced a model-based SHM method considering environmental influences, offering a promising avenue for wind turbine health prediction. Chen, Duffour, and Fromme [19] proposed a two-stage methodology to predict aerodynamic damping, recognizing its correlation with tower vibrations and the impact of motion coupling. Pereira et al. [20] advocated for autonomous data processing in continuous wind turbine monitoring, emphasizing the impracticality of manual analysis. Collectively, these studies contribute to understanding wind turbine dynamics, health monitoring strategies, and aerodynamic damping analysis. However, the number of studies investigating the effect of environmental and operational factors on turbine dynamic characteristics is quite limited, and more detailed studies need to be done on this subject.

The work presented in this paper is centered on the system identification of an operational wind turbine under various operational and environmental conditions, facilitated by the development of a novel Autonomous and Continuous System Identification (ACSI) system. This system utilizes its accelerometers strategically placed at different levels on the wind turbine tower to capture acceleration data, which is subsequently processed through an operational modal analysis method. The resulting modal parameters, in conjunction with operational factors (rotor speed, nacelle direction, pitch angle) and environmental data (temperature, wind speed, wind direction, relative humidity), are stored for further analysis. The primary objective of the paper is to investigate how operational and environmental conditions affect the wind turbine's dynamic characteristics. In general, structural health monitoring systems developed by considering these effects are known to be more reliable. The following tasks are conducted within the research work presented to achieve this goal. A distributed data acquisition system has been designed to record acceleration, temperature, and relative humidity data on the wind turbine. After preprocessing the recorded acceleration data, system identification has been performed using the p-LSCF method. The modal parameters

have been then matched with the operational and environmental factors recorded through the ACSI system's sensors and extracted from the turbine's Supervisory Control and Data Acquisition (SCADA) system. The effects of these factors on the dynamic characteristics of the wind turbine are interpreted by various correlation analyses.

Introduction of the Subject Wind Turbine

The subject structure is a 2.5 MW Horizontal Axis Wind Turbine (HAWT) system (Fig. 1) installed in Izmir/Türkiye [21]. The turbine operates in an area characterized by frequent wind speed and direction variations due to regional climatic conditions. These dynamic weather conditions exert substantial stress on various components of the turbine, including its tower, blades, and connection elements. In the context of contemporary wind energy systems, this turbine can be categorized as a medium-sized unit featuring a hub positioned at an elevation of 90 m above ground level. The wind turbine employs pitch regulation and is equipped with a three-blade rotor configuration. The nacelle, housing the generator and its associated drive train is situated on top of the steel tower. Table 1 provides some of the important technical specifications for the wind turbine.

The tower, a key structural component, is constructed from four circular steel segments made of S355 structural steel, which is bolted to a concrete foundation. The tower's diameter and thickness exhibit variations along its height. While the diameter experiences a gradual reduction in the first three segments, a more significant decrease is introduced in the uppermost segment. It is also important to mention that the wind turbine is erected on stiff soil characterized by relatively high shear velocity (Vs30 = 960 m/s). Therefore, it is assumed that the influence of structure-foundation-soil interaction on the tower dynamics remains minimal and therefore is neglected in the numerical model. Furthermore, the wind turbine is located 2 km from the Güzelbahçe fault line, effectively in a high seismicity zone [22].

Table 1 Properties of the wind turbine

Property	Value
Rated power	2.5 MW
Rated wind speed	12 m/s
Cut-in wind speed	3 m/s
Cut-out wind speed	25 m/s
Rotor speed	9.6–16 RPM
Rotor diameter	90 m
Tower height	78 m
Hub height	90 m
Nacelle mass	91 tons
Rotor mass	55 tons

In normal operational conditions, the oscillation of the wind turbine predominantly originates from wind dynamics. Consequently, it is advantageous to facilitate the estimation of vibration modes by considering the main and secondary wind directions. Specifically, a set of accelerometers should be oriented in alignment with the Main Wind Direction (MWD) which is a region-specific direction. The other set of accelerometers should be oriented perpendicular to the main direction also known as the Secondary Wind Direction (SWD).

The determination of the MWD and SWD required a comprehensive analysis of 4 years' worth of wind data, spanning from January 1st, 2018, to December 31st, 2021, as recorded by the Supervisory Control and Data Acquisition (SCADA) system across 10 wind turbines within the wind farm. This dataset comprises a total of 2,102,400 data

(a) (b)

Fig. 1 **a** The monitored wind turbine and **b** a general view of the wind farm

points, representing 10-min average values. Consequently, the MWD for this region is defined as 11° clockwise from the north.

Numerical Model of the Wind Turbine Tower

The monitored wind turbine consists of 4 main components: a reinforced concrete foundation, a steel tower, a rotor, and a nacelle, which are typical parts of a wind turbine system. For developing numerical models for wind turbines, it is important to consider the eccentricities of the rotor and nacelle with respect to the top center point of the tower, as well as the rotational inertia of the rotor for accurately capturing the turbine's dynamic characteristics [23]. In this study, only the modal parameters of the tower system are studied; therefore, it is decided that the rotor and nacelle are modelled as lump masses but considering their eccentricity and rotational inertia values (Fig. 2).

ANSYS software is used to model the wind turbine system. The model uses solid body finite elements with eight vertices and twenty-four degrees of freedom for the foundation and surface body finite elements with four vertices and twelve degrees of freedom for the tower. The mechanical properties of the material are shown in Table 2. Fixed supports are defined as the boundary conditions at the foundation and soil interface. Soil medium is not modelled. The modal analysis is performed using the linear numerical model, and the tower's first three structural modes are obtained. The natural frequencies and the corresponding mode shapes for the first three tower modes along the fore-aft direction are presented in Fig. 3.

Table 2 Mechanical properties of structural steel and concrete

Structural Steel		Concrete	
Properties	Value	Properties	Value
Yield strength	355 MPa	Compressive strength	25 MPa
Tensile strength	460 MPa	Modulus of elasticity	30 GPa
Modulus of elasticity	210 GPa	Shear modulus	12.7 GPa
Poisson ratio	0.30	Poisson ratio	0.18

In Fig. 2, m_R is the rotor mass, I_{Ry} is the moment of inertia about the axis perpendicular to the rotor plane, I_{Rx} and I_{Rz} are the moment of inertia about the axes parallel to the rotor plane, m_N is the nacelle mass, ez_R, ex_R, ez_N and ex_N are the eccentricity values for the nacelle and rotor with respect to the top center point of the tower. Mass, moment of inertia and eccentricity values are presented in Table 3.

Data Acquisition System

The data acquisition system has two integral components: The hardware component, specifically designed for the introduced wind turbine, records acceleration, temperature, and humidity data from sensors located at various levels of the turbine tower. The data acquisition component has various features. It communicates with the hardware components and ensures the synchronization of data recorded by the turbine system's sensors and the data retrieved from the

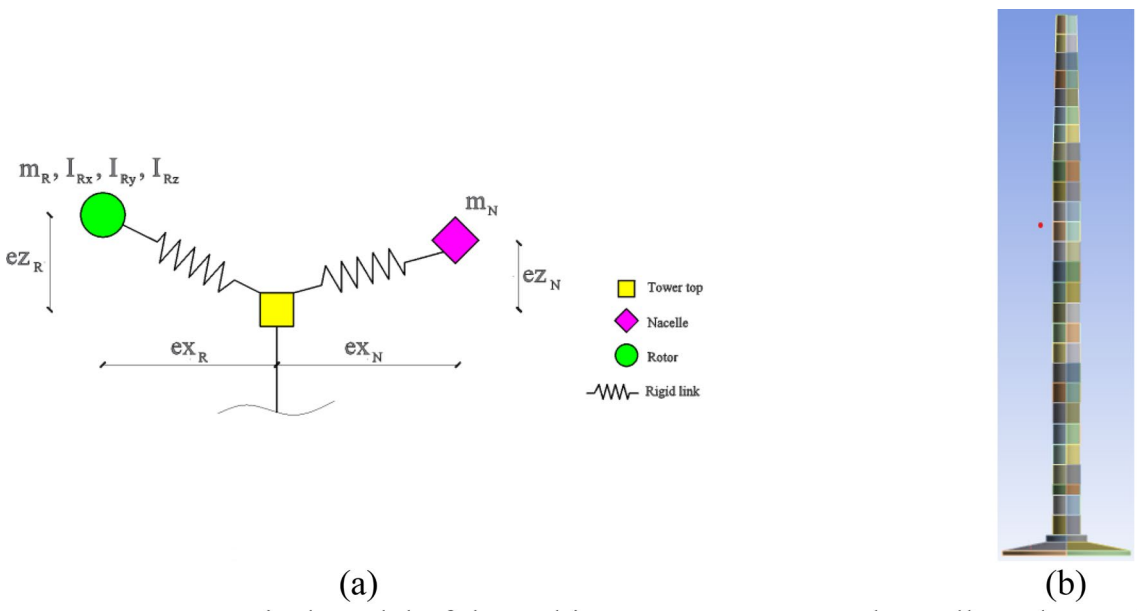

Fig. 2 Numerical model of the turbine tower: **a** rotor and nacelle as lumped masses, **b** foundation and tower as finite elements

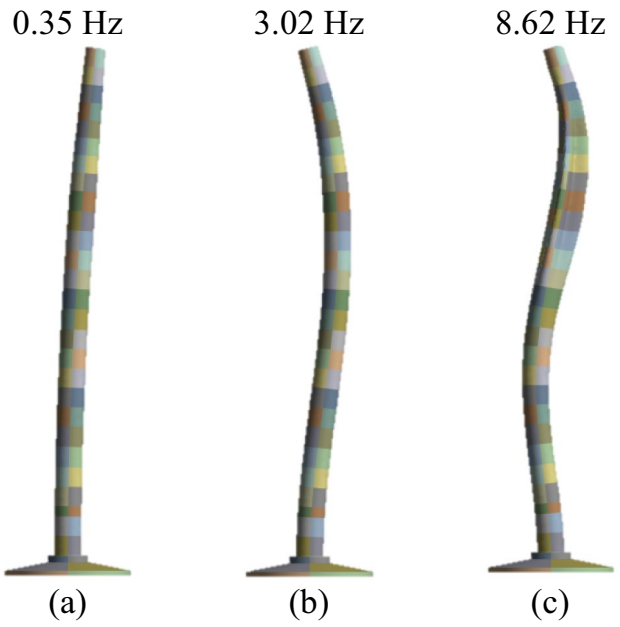

Fig. 3 **a** First, **b** second, and **c** third numerical mode shapes of the wind turbine tower

Table 3 Parameters of the numerical model

Rotor		Nacelle	
Properties	Value	Properties	Value
m_R	55 tons	m_N	91 tons
ez_R	2.00 m	ez_N	0.66 m
ex_R	2.51 m	ex_N	0.72 m
I_{Ry}	1.11E+05 tm^2		
I_{Rx}, I_{Rz}	5.57E+04 tm^2		

SCADA system. Additionally, it performs pre-processing on the acceleration data, repacks all the collected field data, and sends it to the campus environment for subsequent analysis.

Hardware

The wind turbine tower has a total height of 78 m and includes walkable platforms at 20-m intervals. At the foundation level, three uni-axial accelerometers and one tri-axial accelerometer are deployed for recording both horizontal and vertical acceleration. On the other levels, which are located at 20, 40, 60, and 78 m, two uniaxial accelerometers are positioned horizontally (Fig. 4a) to measure horizontal acceleration along two perpendicular directions, namely the MWD (x) and SWD (y) directions (Fig. 4b). These accelerometers possess high-resolution and low-noise characteristics (Table 4). Additionally, temperature sensors are placed at three levels within the tower: the foundation, 40 m, and 78 m levels. Furthermore, the relative humidity sensors are positioned inside the tower at two levels, one at the foundation and the other at the 78 m level (Fig. 4c).

The data acquisition scheme set forth for this research work has three constituent parts/stations: switchyard, turbine, and campus. The network infrastructure connecting these stations is designed to facilitate continuous communication among these stations, ensuring synchronous data transfer. The network is configured to enable data transfer from the SCADA system located at the switchyard station via an industrial PC, extracting the data behind a firewall. Point-to-point (P2P) antennas are installed at both the switchyard and the turbine stations, providing internet service for the turbine side via the switchyard's modem and enabling data transfer between the two. An 8-port Ethernet switch connected to the computer and the chassis at each level within the tower, enabling communication among all the hardware components deployed at the tower. A robust data flow between the turbine and the campus has been established via the Internet using a VPN service (Fig. 5).

Data Acquisition Software

Multiple LabVIEW codes have been developed in the switchyard, turbine, and campus stations to manage the data collection process, post-process the streaming acceleration data for later use in subsequent analysis and send all the data to the campus environment in a coordinated manner. The codes developed perform the following step by step procedure:

1. The codes acquire various sensor data (14 channels of acceleration, 3 channels of temperature, and 2 channels of humidity) from the wind turbine simultaneously.
2. Environmental and operational data are transmitted from the switchyard to the wind turbine using P2P antennas, enabling internet access to the data acquisition system on the turbine via remote connection.
3. Acceleration data, environmental data (i.e., temperature, wind speed, relative humidity, and wind direction), and operational data from the turbine's SCADA system (i.e., rotor speed, nacelle direction, pitch angle, and actual power) are synchronized.
4. The acceleration data is pre-processed for system identification, which involves filtering, decimation, and detrending.
5. Data is continuously saved in packets of user-set desired duration, which are subsequently transferred to the campus environment and stored in Network-Attached Storage (NAS) devices for further analysis.

Data from the tower and the SCADA system was recorded continuously for 7 months. Within this period, acceleration data was recorded at a sampling frequency of 2048 Hz. For

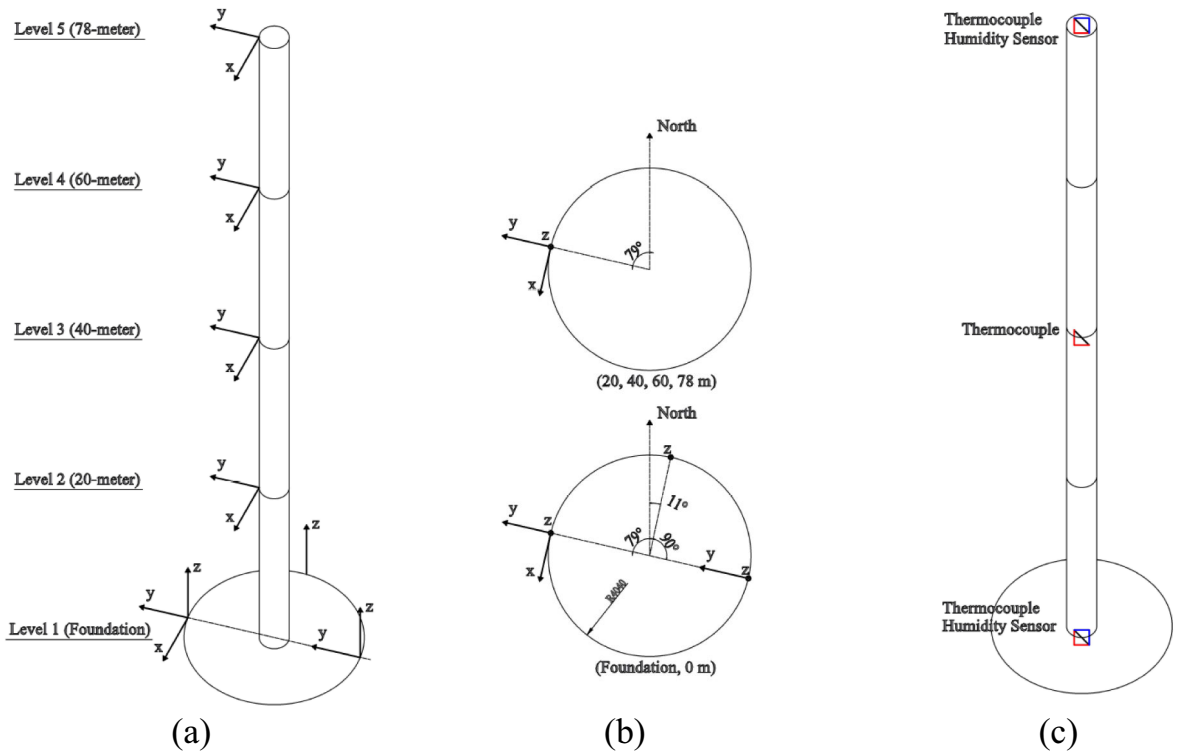

Fig. 4 **A** Accelerometer layout along the turbine tower, **b** accelerometer layout in the plan view, **c** thermocouple and relative humidity sensor layout along the tower

Table 4 Technical specifications of the accelerometers

Acc. Range (g)	±5
Sensitivity (mV/g)	540
Frequency Range (Hz)	0–700
Noise (μg/$\sqrt{\text{Hz}}$)	0.1
Bias Temperature (mg/°C)	17
Shock Survivability (g)	2500
Operating Voltage (V)	5–20

each of the recorded 600 s acceleration dataset, a low-pass filter with a corner frequency of 30 Hz was applied. Then, a detrending process was implemented, and the data was down-sampled to 256 Hz for further analysis and storage.

Autonomous and Continuous System Identification

To investigate the effect of operational and environmental factors on the dynamic characteristics of an operational wind turbine, an Autonomous and Continuous System Identification (ACSI) system has been developed. This system automates the entire system identification phase by eliminating the need for user intervention. The key features of this autonomous system are summarized as follows:

1. The system continuously monitors the directory where data files are stored and reads new files for further processing.
2. The p-LSCF method is employed to automatically extract modal parameters from the acceleration data by using a stabilization diagram based on pre-defined stabilization criteria.
3. The stabilization diagram constructed for each 600-s-long acceleration data is used automatically to estimate modal parameters, i.e., natural vibration frequencies, damping ratios, and mode shapes.
4. Operational and environmental conditions corresponding to the modal parameters estimated in the previous step are computed by simply averaging the same 600-s-long data segments.
5. The estimated modal parameters are matched with the operational and environmental conditions, and the results are stored, including date and time stamps for reference.

At the 3rd step of the process, when examining the stabilization diagrams calculated from data recorded under various operational and environmental conditions, it is expected

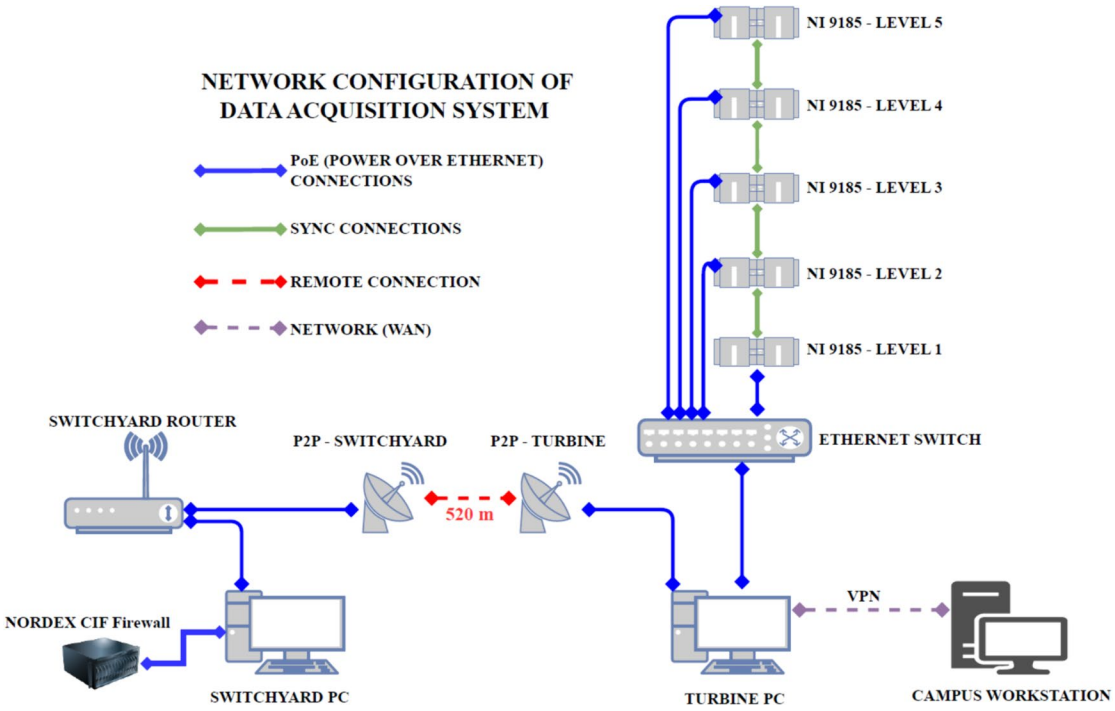

Fig. 5 Network configuration of the data acquisition system

that the modes will be slightly shifted in frequency due to varying conditions. Additionally, some non-physical modes may also appear in stabilization diagrams. A procedure has been devised to ensure the accurate selection of the physical modes from a diagram. This procedure checks all stable poles (modes) that meet the predefined criteria. If three stable modes at a specific frequency with different order numbers are found to fall within a narrow frequency range set by the user-specified small tolerance value, the mode with the lowest order number is designated as the physical mode for the identified tower system. No further assessment is made regarding the other poles for that specific frequency.

The autonomous mode selection process is depicted in Fig. 6 as a flowchart. Selected physical modes, indicated with red circles, using the autonomous mode picking procedure using a stabilization diagram are shown in Fig. 7. It can be seen from the figure that the p-LSCF method provides very clean stabilization diagrams, thereby simplifying the autonomous selection of the physical modes.

Effects of Operational and Environmental Conditions on Modal Parameters

Operational and Environmental Conditions

A total of 13,277 non-uniformly sampled data files, each spanning 600 s, were used to assess the effect of operational and environmental conditions on the dynamic characteristics of the wind turbine. These recordings were made between July 7, 2022 and February 7, 2023 spanning both winter and summer periods but in an uniform way in time due to technical difficulties encountered with the system. The data was systematically processed using the ACSI system, encompassing a range of operational and environmental conditions enabling a comprehensive correlation analysis.

Figure 8 shows wind speed, temperature, relative humidity, wind, and nacelle directions histograms from the 7-month-long data.

During the recording period, wind speeds typically ranged from 1 to 15 m/s, with an average wind speed of 7.2 m/s and a maximum recorded speed of 23.2 m/s, which was still below the wind turbine's cut-out wind speed (see Table 1). Consequently, there were no emergency shutdowns due to very high wind speeds. The corresponding dataset primarily reflects outside temperatures, since the temperature readings from the thermo-couples at 0, 40, and 80 m within the tower are very close to the outside temperature values recorded by the SCADA system. The temperature readings range between 0 and 35 °C, with temperature values concentrated between 9–19 and 24–30 °C temperature intervals. For the relative humidity, the collected data primarily represents inside conditions at the 80-m level. It is noted that the values recorded at this level are similar to those at the 0-m level. Due to the regional climate conditions, most recordings were

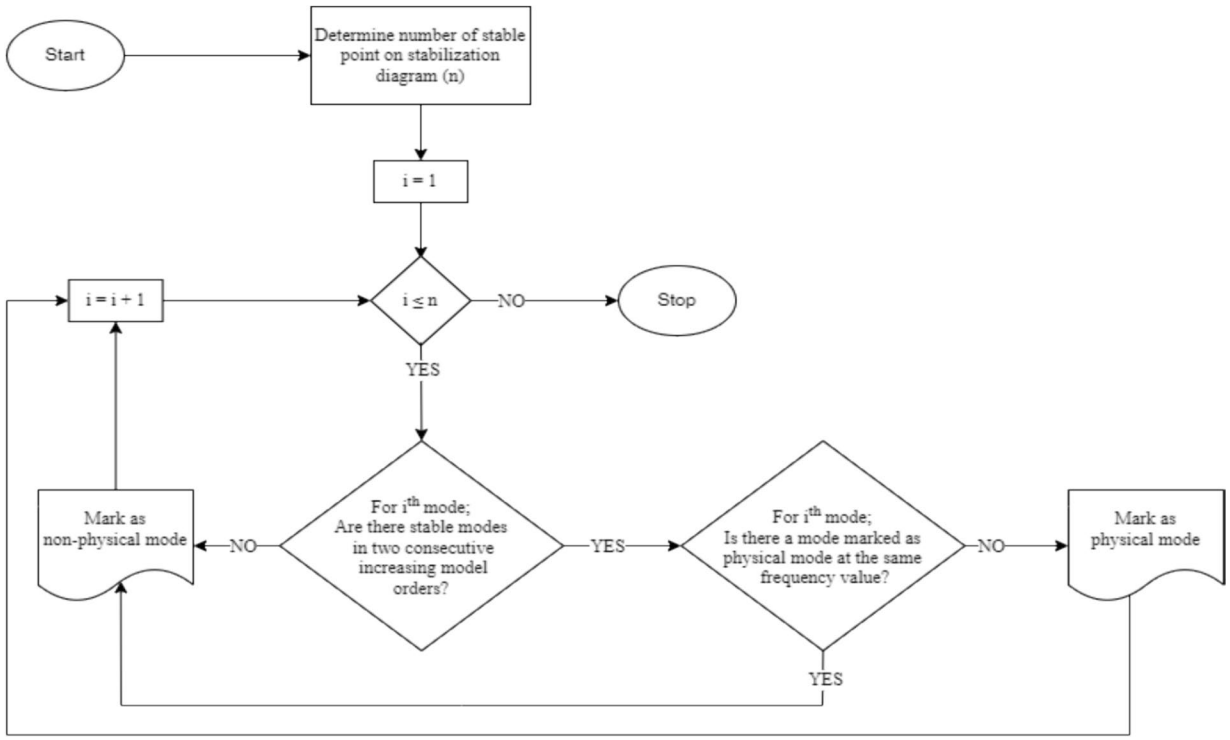

Fig. 6 Autonomous mode picking procedure

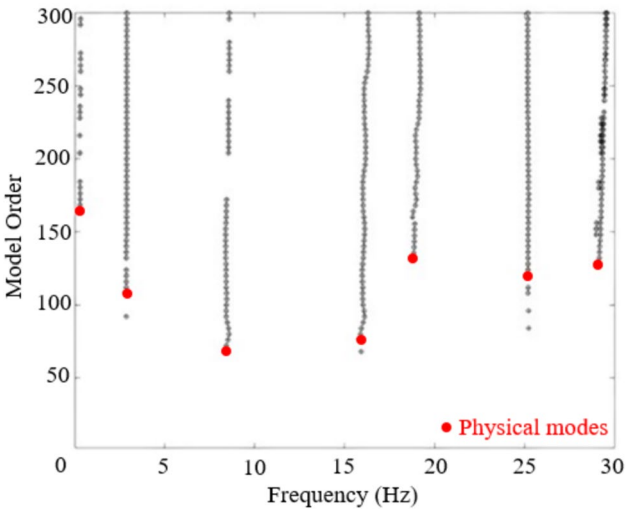

Fig. 7 Selected physical modes using autonomous mode picking procedure

made in humid environment, with relative humidity values ranging between 18 and 82%.

Regarding the wind and nacelle directions, it is worth noting that 0° represents the exact north direction, and the positive rotational direction is in clockwise direction. As anticipated, a higher percentage of data was recorded while the nacelle was in the Main Wind Direction (MWD) compared to the other directions. Typically, the nacelle aligns itself with the wind direction for efficient energy production, guided by the wind turbine's control system. Consequently, wind and nacelle directions generally show similar orientations. However, some differences can be observed in Fig. 8b, d, reflecting instances when the wind direction had not been stable enough for the turbine's control system to adjust the nacelle to the wind direction.

The histograms for the rotor speed and pitch angle are presented in Fig. 9. It can be seen from the figure that the operational conditions can be categorized into three distinct states, namely passive, semi-active, and active states. The modal parameters of the wind turbine can vary based on its operational state. Therefore, for a better understanding of the turbine's dynamic characteristics, all recorded 600-s-long datasets have been classified into three categories based on the rotor speed of the wind turbine:

i. **Passive state:** Occurs when the wind speed is in 0–3 m/s range. The rotor brakes are engaged in this state, and the rotor speed is maintained at 0 RPM. The turbine remains idle meaning that no energy is generated. However, in some instances, the brakes may not be engaged, causing the turbine blades to rotate very slowly at speeds ranging from 0 to 1 RPM.
ii. **Active state:** Occurs when the wind speed exceeds 3 m/s. The turbine transitions into an active state,

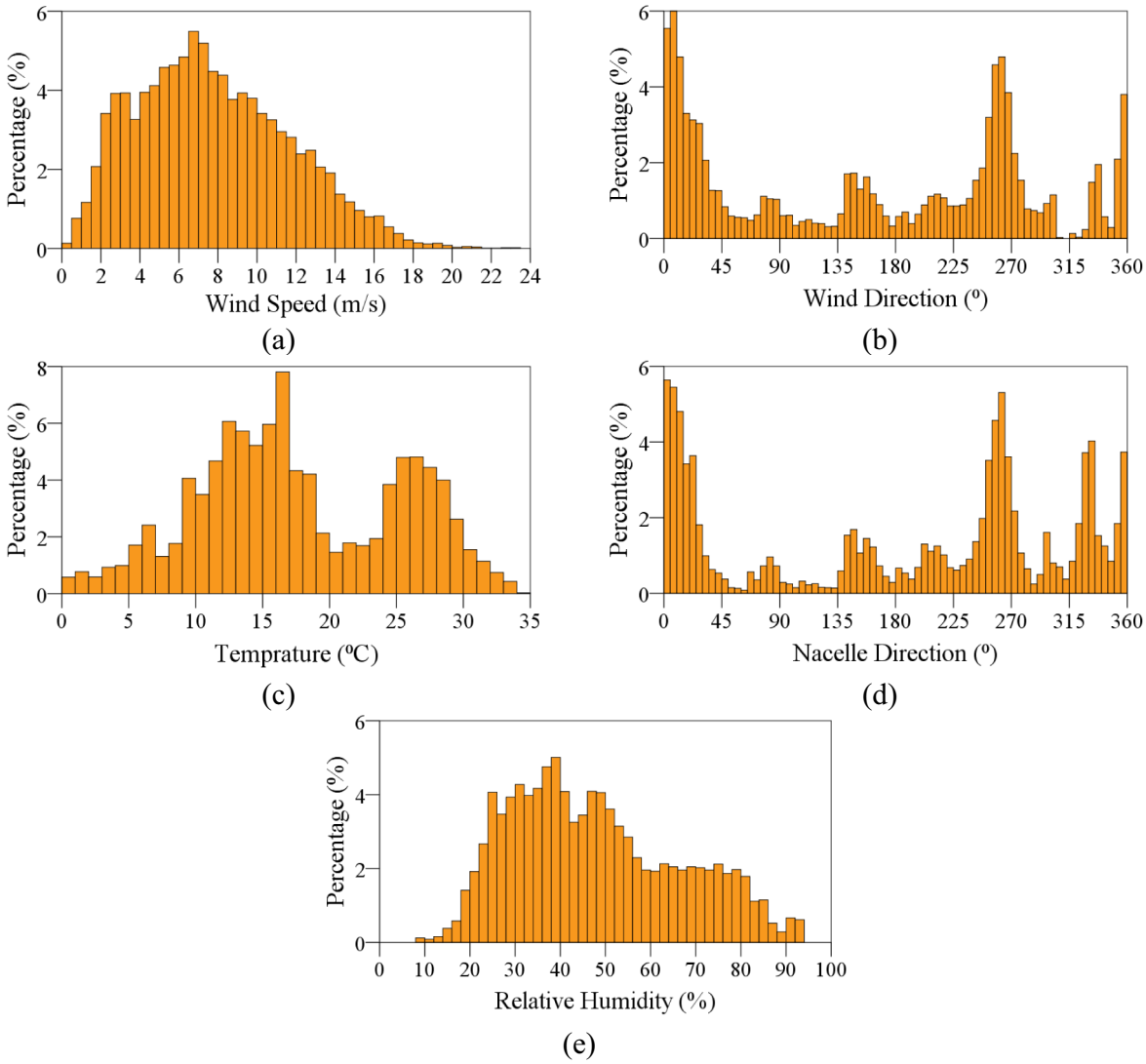

Fig. 8 **a** Wind speed, **b** wind direction, **c** temperature, **d** nacelle direction, and **e** relative humidity histograms

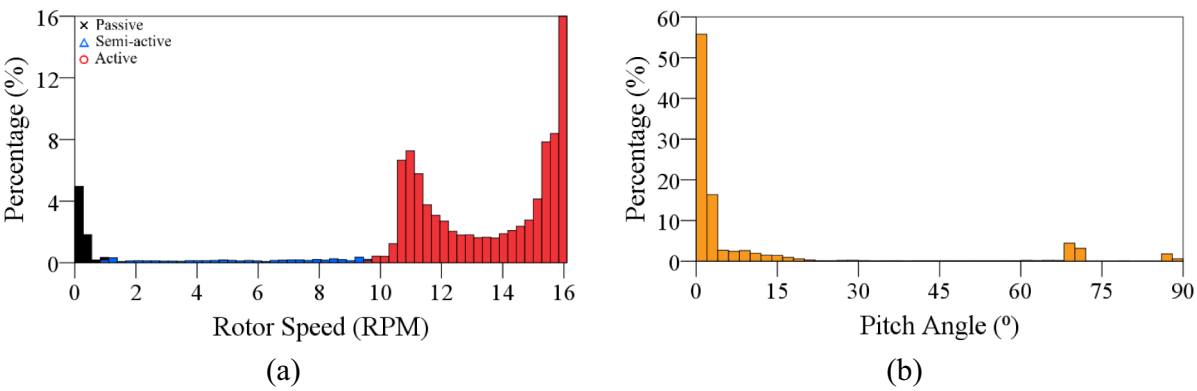

Fig. 9 **a** Rotor speed and **b** pitch angle histograms

initiating energy production. In this state, the wind turbine's rotor operates at a range of 9.6–16 RPM.

iii. **Semi-active state:** Occurs when the turbine switches between active and passive states. In semi-active states, the rotor speed fluctuates between 1 and 9.6 RPM.

The turbine's rated wind speed is 12 m/s. Rotor speed increases with higher wind speeds within the 3–12 m/s speed range. Beyond the rated wind speed, the turbine's controller maintains the rotor speed at a constant 16 RPM, producing maximum energy. The turbine control system adjusts the pitch angle of the rotor blades to achieve a constant angular velocity. A pitch angle of 0° exposes the entire blade surface to the wind (i.e., maximum area exposure), while increasing the pitch angle decreases the effective wind surface of the blades, leading to slower angular velocities. In passive states, the pitch angle is not controlled therefore, it is set to random pitch angle values such as 0° or around 70–72° and 85–90°.

Relationship Between Operational and Environmental Conditions

In order to systematically assess the influence of operational and environmental factors on the turbine dynamics, it is crucial to establish a clear understanding of the relationship between the aforementioned operational and environmental conditions, which serves as a critical basis for analyzing and interpreting the data, allowing for deeper insights into how various factors impact the turbine dynamics.

The relationships between wind speed/rotor speed, wind speed/pitch angle, and rotor speed/pitch angle are shown in Fig. 10.

The cut-in, rated, and cut-out speeds of the wind turbine are 3 m/s, 12 m/s, and 25 m/s, respectively (also refer to Table 1). Based on these speed limits (V_{wind}), the turbine's operation can be divided into four distinct regions:

- $0\ m/s \leq V_{wind} < 3\ m/s$: In this range, the turbine remains inactive and does not generate power. The rotor's angular velocity is maintained at 0 RPM, and the power output is 0 kW. The pitch angle of the blades may vary.
- $3\ m/s \leq V_{wind} < 12\ m/s$: As wind speed increases while staying in this range, both rotor speed and actual power output increase as well. The pitch angle stays constant at 0°, allowing efficient energy capture.
- $12\ m/s \leq V_{wind} < 25\ m/s$: The rotor speed is maintained at a constant 16 RPM (the rated rotor speed) in this range. As wind speed increases, the controller kicks in and starts controlling the pitch angle. The pitch angle of the blades increases exposing, smaller blade area to ensure that the rotor speed remains constant. The wind turbine produces 2.5 MW of rated power.

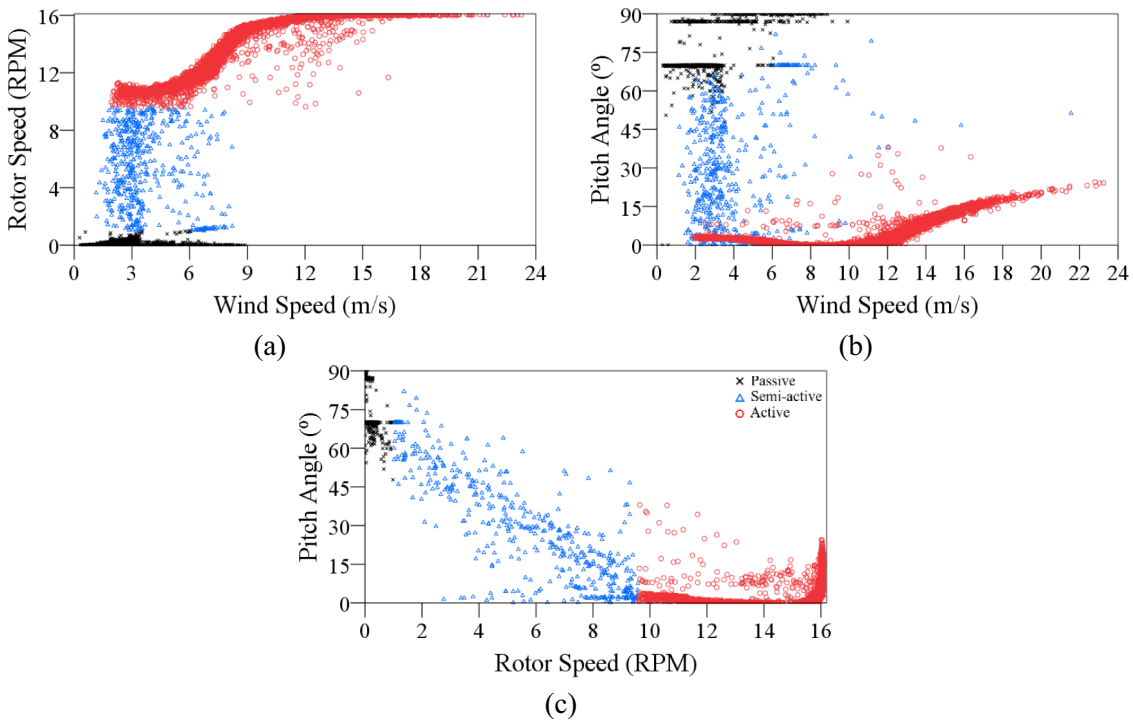

Fig. 10 Relationships between **a** wind speed/rotor speed, **b** wind speed/pitch angle, **c** rotor speed/pitch angle

- 25 m/s ≤ V_{wind}: The system's controller gradually stops the rotor as wind speed exceeds 25 m/s to prevent structural damage caused by excessive wind speeds and, therefore, forces. The pitch angle is set at 90° to minimize wind loads on the blades and the rotor, effectively shutting down power generation.

It is important to note that the transition between active and passive cases requires the wind speed to remain above or below a specific cut-in wind speed for a particular duration. Note that some exceptional points in Fig. 10 may result from the intervention of the turbine control system or maintenance activities.

Effects of Operational and Environmental Conditions on the Estimated Modal Frequencies

The ACSI system identified three vibration modes using the autonomous operational modal analysis process. The modal parameters estimated using the data recorded in the MWD and SWD directions are very similar. Therefore, only the results of the analyses conducted in the MWD direction will be presented in the study. The mean values of the estimated modal frequencies from the recorded data are presented in Table 5 with their numerical counterparts calculated using the numerical model of the wind turbine. The estimated frequencies differ from the main excitation frequencies of the turbine rotor, namely the 1p and 3p frequencies. The 1p frequency corresponds to the excitation frequency based on the number of revolutions of the rotor per second, which aligns with the rated rotor speed of 16 RPM, equivalent to 0.27 Hz. The 3p frequency represents the excitation frequency caused by the passage of all three rotor blades near the turbine tower, which is equal to 0.8 Hz. It is worth noting that these three modes have been captured in varying number of times across 13,277 data sets. Due to the low-frequency response characteristics of the accelerometers used in the project, the vibration mode at 0.35 Hz is the mode which is captured the least number of times. Although modal frequency estimations are more reliable than the other estimated modal parameters (i.e., mode shapes and damping ratios), it is still important to recognize that the wind turbine's modal frequencies can be affected by various operational and environmental conditions.

Table 5 Estimated modal frequencies and their numerically calculated counterparts

Mode	Estimated	Numerical	Difference
1st bending	0.35 Hz	0.35 Hz	< 0.1%
2nd bending	3.00 Hz	3.02 Hz	0.7%
3rd bending	8.29 Hz	8.62 Hz	4.0%

The relationship between the estimated frequencies of the first three structural modes and the rotor speed is shown in Fig. 11. The vertical axes in all plots presented in this section depict the normalized frequency shift value which is calculated using Eq. (1).

$$f_{ns} = \frac{\bar{f} - \bar{f}_{ave}}{\bar{f}_{ave}} \tag{1}$$

where $\bar{f}$ is the estimated frequency for each case, $\bar{f}_{ave}$ is the mean value of the estimated modal frequencies and f_{ns} is the normalized frequency shift for each case.

For the modal frequency at 3.00 Hz, there is a positive correlation between frequency estimates and rotor speed for active cases only (r = 0.582 [Pearson correlation coefficient] and p ≤ 0.001 [significance level]). In addition, there is a decrease (a drop in values) in the frequency estimations when the rotor speed reaches around 16 RPM (the very end part of Fig. 11b). This decrease (or drop) in the estimated frequencies is attributed to the pitch angle parameter which is discussed later in the paper (the effects of pitch angle and wind speed factors are discussed (Figs. 12 and 15)). As mentioned earlier, the turbine's controller starts to increase the pitch angle to maintain a constant rotor speed of 16 RPM after reaching the rated wind speed and beyond. This adjustment in pitch angle affects the wind loads on the rotor blades and therefore the dynamics of the wind turbine tower. For the frequency estimates at 0.35 Hz and 8.29 Hz, no clear correlation is observed between the frequency and the rotor speed.

Figure 12 shows the relationship between wind speed and frequency estimates of the three modes.

For the frequency at 3.00 Hz, there is a positive correlation between the wind speed and modal frequencies up to the rated wind speed of 12 m/s (r = 0.726 and p ≤ 0.001). As wind speed continues to increase, the estimated frequencies tend to increase, indicating that the wind conditions have a significant effect on the turbine tower's dynamics. The frequency estimations start to decrease beyond the rated wind speed value (r = 0.427 and p < 0.001). This can be attributed to increasing pitch angles enforced by the turbine controller to maintain a constant rotor speed of 16 RPM, significantly reducing wind loads on the rotor. For the modes at 3.00 Hz and 8.29 Hz, as wind speed increases the scatter in the frequency estimations is reduced. This suggests that at higher wind speeds, contributions from these modes to the tower's overall dynamics are more pronounced.

Figure 13 shows the relationship between measured temperatures and frequency estimates for the first three modes.

It can be observed that the frequency estimations for the modes at 3.00 Hz and 8.29 Hz decrease slightly with increasing ambient temperature (r = -0.095, p < 0.001 and r = -0.274, p < 0.001, respectively). As the temperature

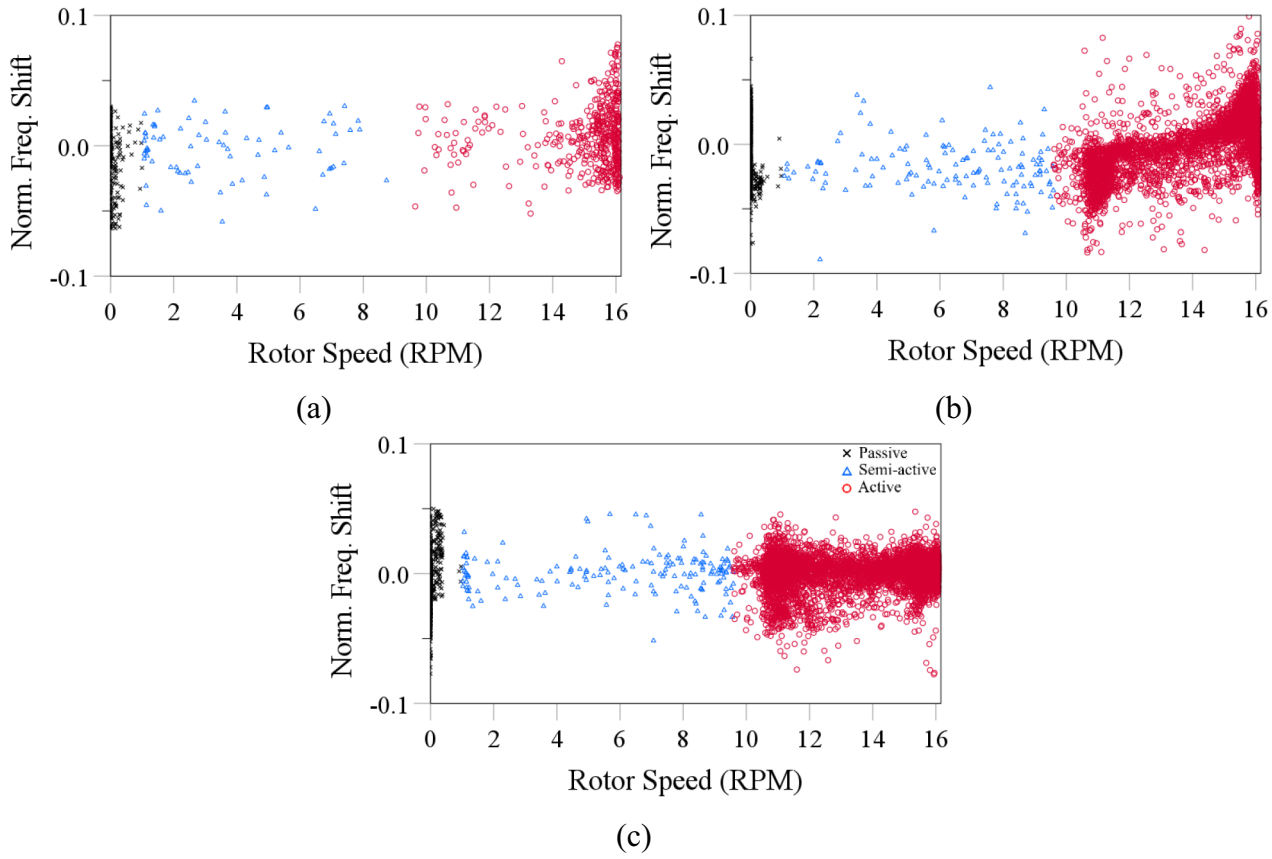

Fig. 11 Relationships between rotor speed and frequency estimates at **a** 0.35 Hz, **b** 3.00 Hz, and **c** 8.29 Hz

rises, the values of the estimated frequencies for the tower decrease.

Figure 14 shows the relationship between measured relative humidity and frequency estimates for the first three modes.

As relative humidity values increase, the modal frequency at 8.29 Hz tends to slightly increase in value ($r = 0.150$ and $p < 0.001$), while the one at 3.00 Hz experiences a slight decrease in value ($r = -0.136$ and $p < 0.001$). However, for the frequencies at 0.35 Hz, there is no clear and consistent trend between the measured relative humidity and the frequency estimations.

Figure 15 shows the relationship between the measured pitch angles of the rotor blades and the frequency estimates.

As noted earlier, the wind turbine's controller increases the pitch angle of the rotor blades to maintain a constant rotor speed of 16 RPM after reaching the rated wind speed of 12 m/s. This change in pitch angles results in reduced wind loads on the rotor due to a decrease in the blades' surface area. Consequently, the decrease in thrust force on the wind turbine contributes to a decrease in frequency estimations for the mode estimated at 3.00 Hz. Moreover, the data shows a significant reduction in frequency scattering after 5° pitch angle. To give an idea about the reduction scattering, for the mode estimated at 3.00 Hz, the standard deviation of normalized frequency shift is 0.030 for the 3° (± 0.5) pitch angle, and 0.011 for the 15° (± 0.5) pitch angle. Similarly, for the mode estimated at 8.29 Hz, the standard deviation of normalized frequency shift at the 3° (± 0.5) pitch angle is 0.007 which is notably lower than the value calculated at the 15° (± 0.5) which is 0.014. For the frequency estimated at 3.00 Hz, the passive and semi-active cases exhibit the same trend as in the active cases. In contrast, the frequency values estimated for the passive and semi-active cases exhibit a high degree of scattering for modes estimated at 0.35 Hz and 8.29 Hz. These findings highlight how the pitch angle adjustment influences the turbine dynamics leading to more stable and less scattered frequency estimations in certain pitch angle values.

No clear trend has been observed between the estimated modal frequencies and the nacelle or wind directions. This lack of trend suggests that the modal frequencies of the wind turbine are not significantly affected by the nacelle or wind directions due to the axisymmetric nature of the tower cross-section with respect to the vertical axis.

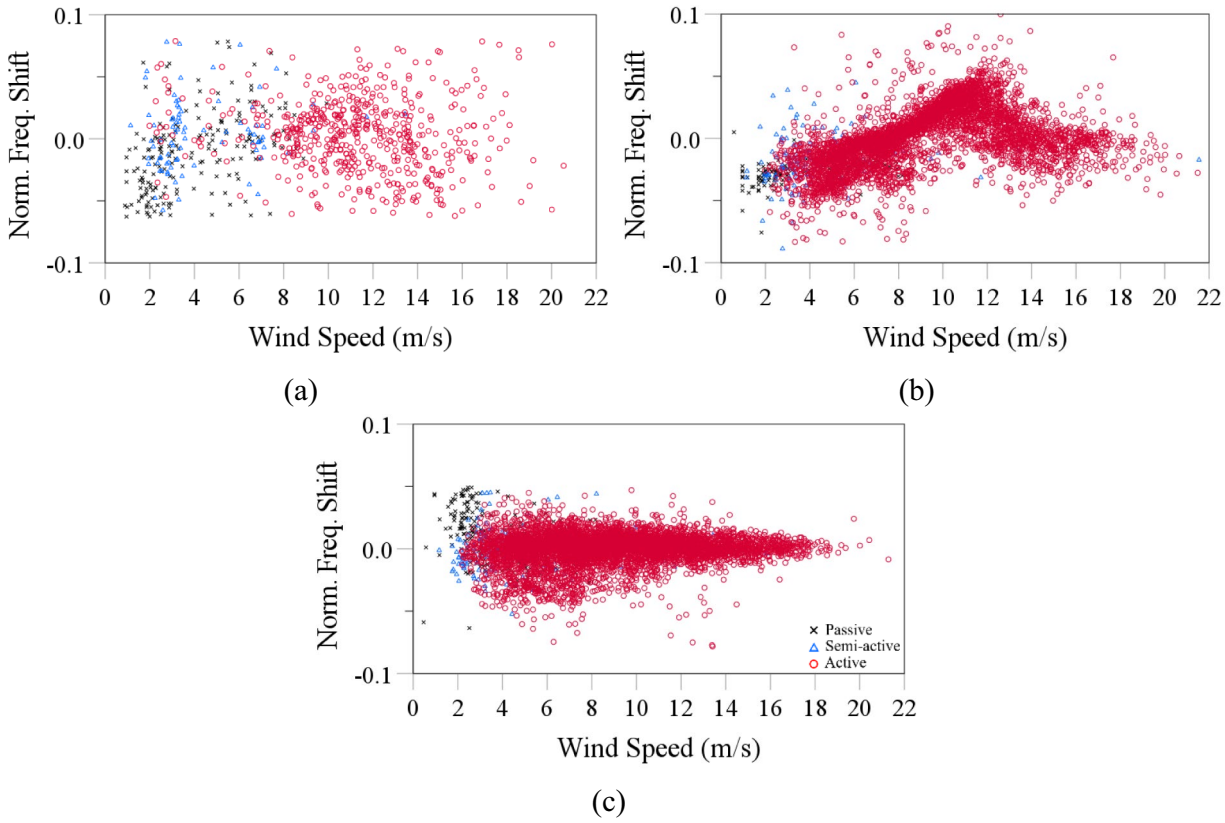

Fig. 12 Relationships between wind speed and frequency estimates at **a** 0.35 Hz, **b** 3.00 Hz, and **c** 8.29 Hz

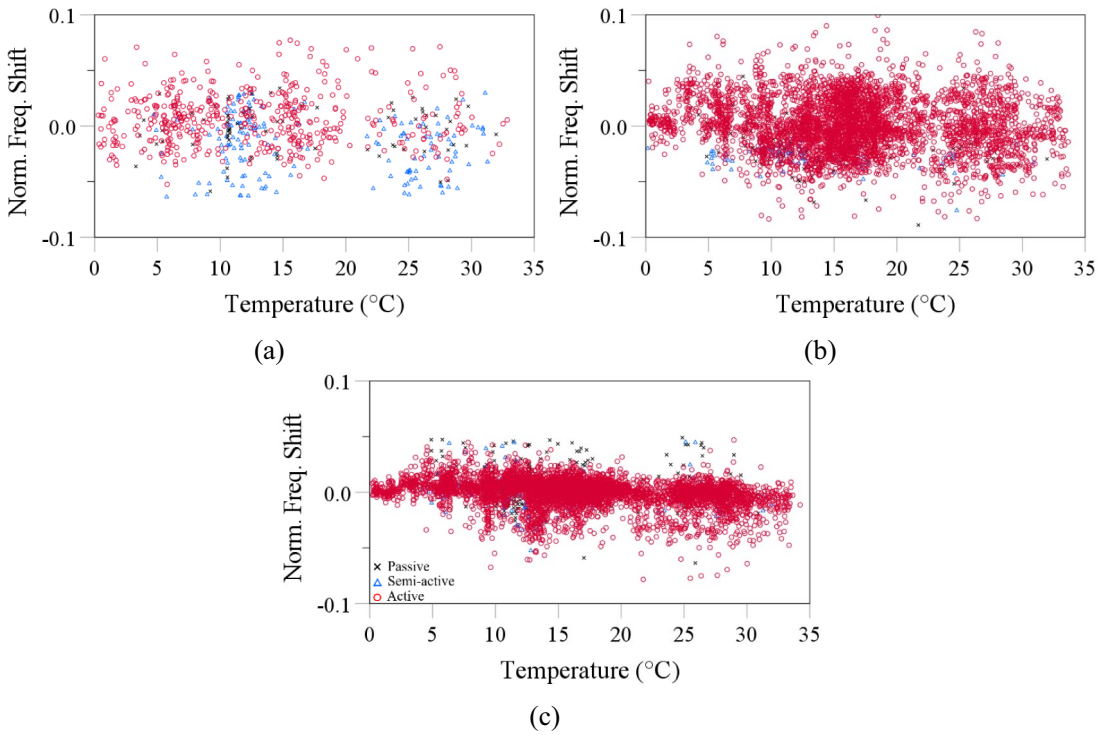

Fig. 13 Relationships between temperature and frequency estimates at **a** 0.35 Hz, **b** 3.00 Hz, and **c** 8.29 H

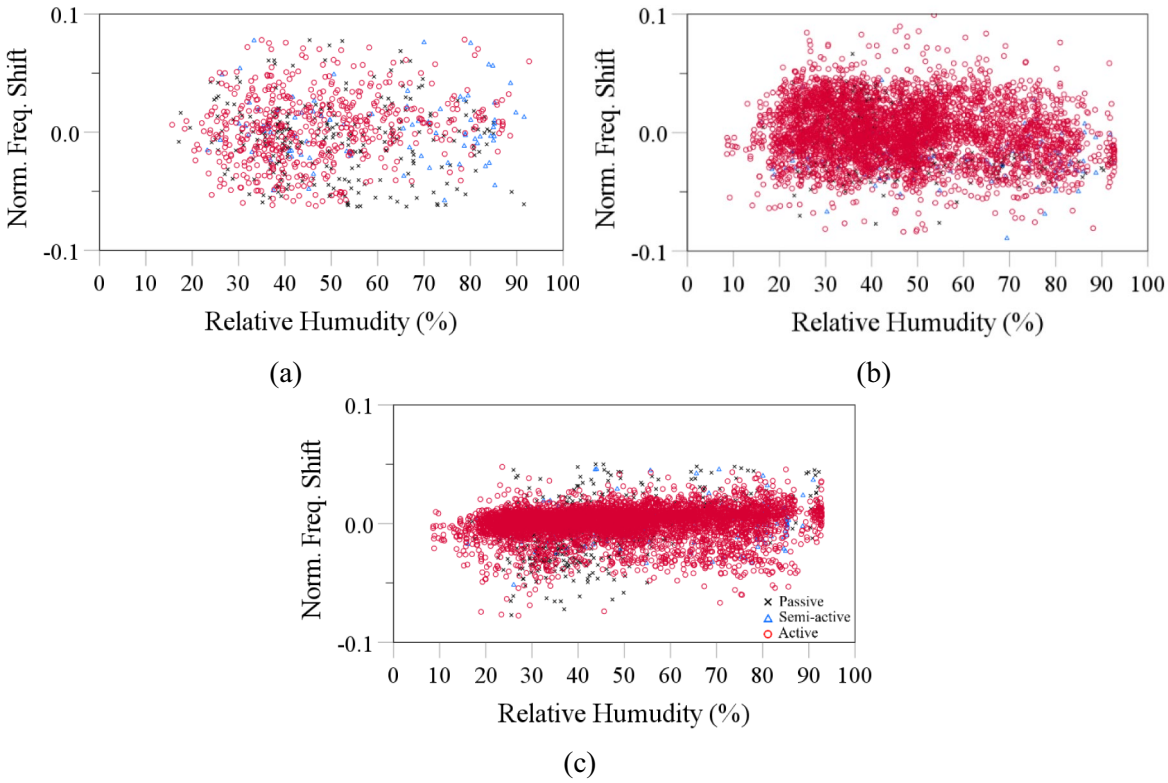

Fig. 14 Relationships between relative humidity and frequency estimates at **a** 0.35 Hz, **b** 3.00 Hz, and **c** 8.29 Hz

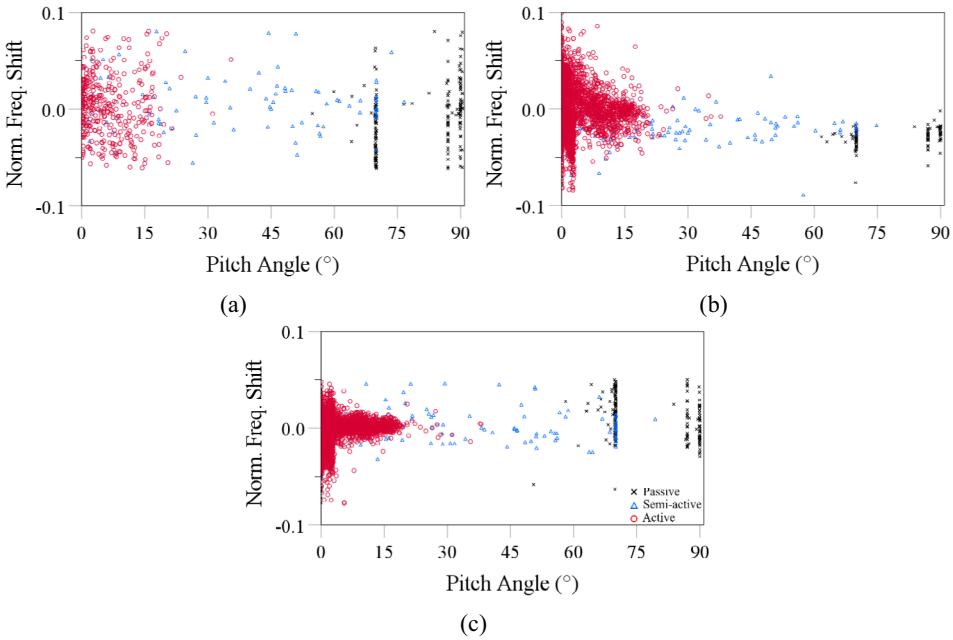

Fig. 15 Relationships between the pitch angle and frequency estimates at **a** 0.35 Hz, **b** 3.00 Hz, and **c** 8.29 Hz

The Effect of Operational and Environmental Conditions on Damping Ratios

In the literature, it is documented that the damping ratios of vibration modes are primarily affected by rotor speed [24–26]. This influence is typically attributed to aerodynamic damping resulting from the interaction of turbine blades as they pass near the tower. Given this background, the results obtained in this work demonstrate the

relationship between the damping estimates and operational and environmental factors.

The relationship between damping estimates and rotor speed is shown in Fig. 16.

Damping ratios have been estimated up to 8%, 8%, and 6% for the frequency estimates at 0.35 Hz, 3.00 Hz, and 8.29 Hz, respectively. It is observed that damping estimates tend to increase as rotor speed increases for the frequency estimates at 3.00 Hz ($r = 0.354$ and $p < 0.001$) and 8.29 Hz ($r = 0.455$ and $p < 0.001$). This increase is due to aerodynamic damping effect, which contributes significantly to the total damping of the turbine. For the frequency estimates at 0.35 Hz, no clear relationship has been identified between the damping ratio and the rotor speed.

The relationship between damping estimates and wind speed is shown in Fig. 17.

The scattering around the mean of the damping estimates is generally higher for the passive cases than the active cases, except for the frequency estimates at 3.00 Hz. This difference can be explained by the increased wind speed resulting in faster rotor rotation, which in turn elevates the excitation level of the structure, eventually leading to more reliable modal parameter estimations. In the passive cases, low signal-to-noise ratio results in increased uncertainty in estimation results. The effect of low signal-to-noise ratio is particularly prominent in the case of damping ratios. A clear positive correlation is observed between the wind speed and damping estimates for the active cases ($r = 0.324$, $r = 0.463$, and $r = 0.446$ for the mode estimated at 0.35 Hz, 3.00 Hz, and 8.29 Hz respectively with $p < 0.001$). Furthermore, a significant jump in the damping estimates is noticeable, increasing from approximately 2.00% to around 3.70% at the rated wind speed for the frequency estimates at 3.00 Hz.

The relationship between damping estimates and temperature is shown in Fig. 18.

No clear correlation is observed between the temperature and damping estimates. The absence of correlation suggests that the damping characteristics of the turbine's vibrational modes are not affected by changes in the ambient temperature. The absence of correlation suggests that the damping characteristics of the turbine's vibrational modes are not affected by changes in the ambient temperature.

The relationship between damping estimates and relative humidity is shown in Fig. 19.

For the modal frequencies at 3.00 Hz and 8.29 Hz, the damping estimates tend to slightly decrease with increased ambient humidity, particularly for active cases. No clear correlation is observed between relative humidity and damping ratios for the modal frequency estimates at 0.35 Hz.

The relationship between damping estimates and pitch angle is shown in Fig. 20.

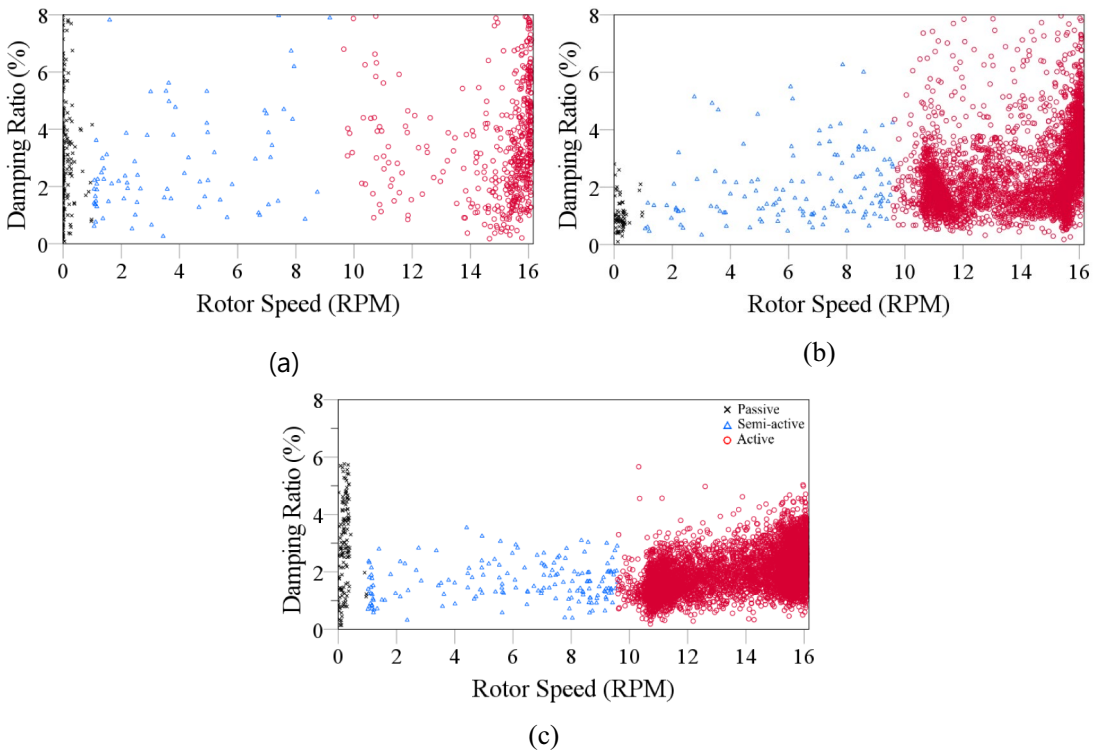

Fig. 16 Relationships between the rotor speed and damping estimates for the frequency estimates at **a** 0.35 Hz, **b** 3.00 Hz, and **c** 8.29 Hz

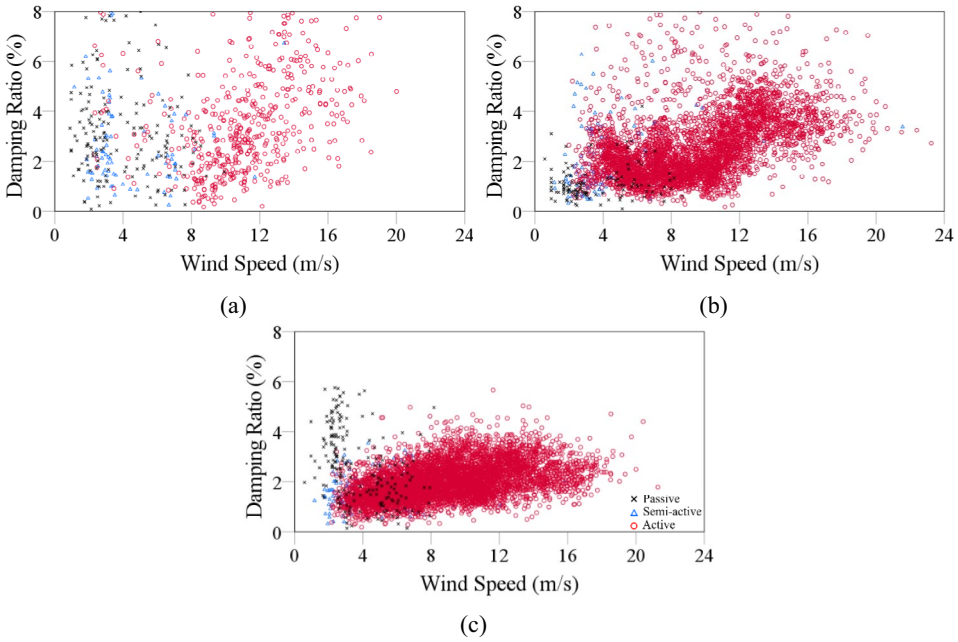

Fig. 17 Relationships between the wind speed and damping estimates for the frequency estimates at **a** 0.35 Hz, **b** 3.00 Hz, and **c** 8.29 Hz

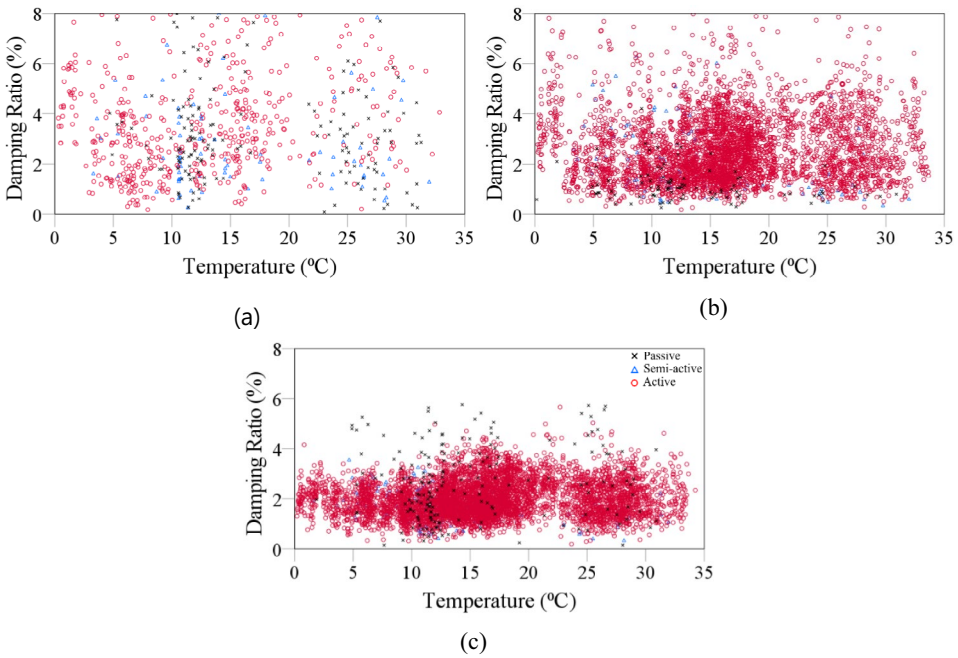

Fig. 18 Relationships between the temperature and damping estimates for the frequency estimates at **a** 0.35 Hz, **b** 3.00 Hz, and **c** 8.29 Hz

Like frequency estimates, there is a significant reduction in damping scattering after 5° pitch angle. While the scattering of the damping estimates is relatively high for the frequency estimated at 3.00 Hz as compared to the ones at 8.29 Hz, there is a notable scattering of frequency values observed for the passive and semi-active cases, particularly for modes estimated at 0.35 Hz and 8.29 Hz modal frequency. No clear correlation has been identified between the damping estimates and the nacelle or wind directions. The absence of a clear correlation suggests that the damping characteristics of the turbine's vibrational modes are not significantly affected by the orientation of the nacelle or the prevailing wind direction.

Effect of Operational and Environmental Conditions on Mode Shapes

In order to assess the effects of operational and environmental conditions on the estimated mode shapes, the following procedure is devised to determine the principal mode shapes:

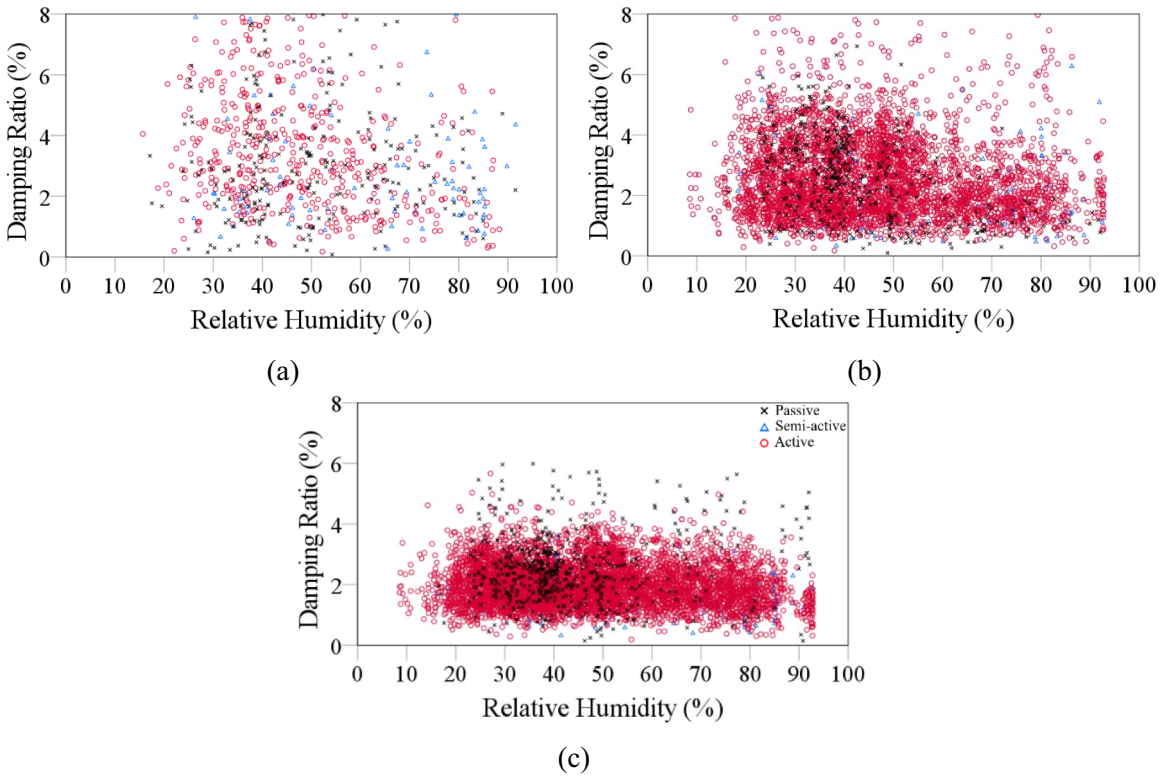

Fig. 19 Relationships between relative humidity and damping estimates for the frequency estimates at **a** 0.35 Hz, **b** 3.00 Hz, and **c** 8.29 Hz

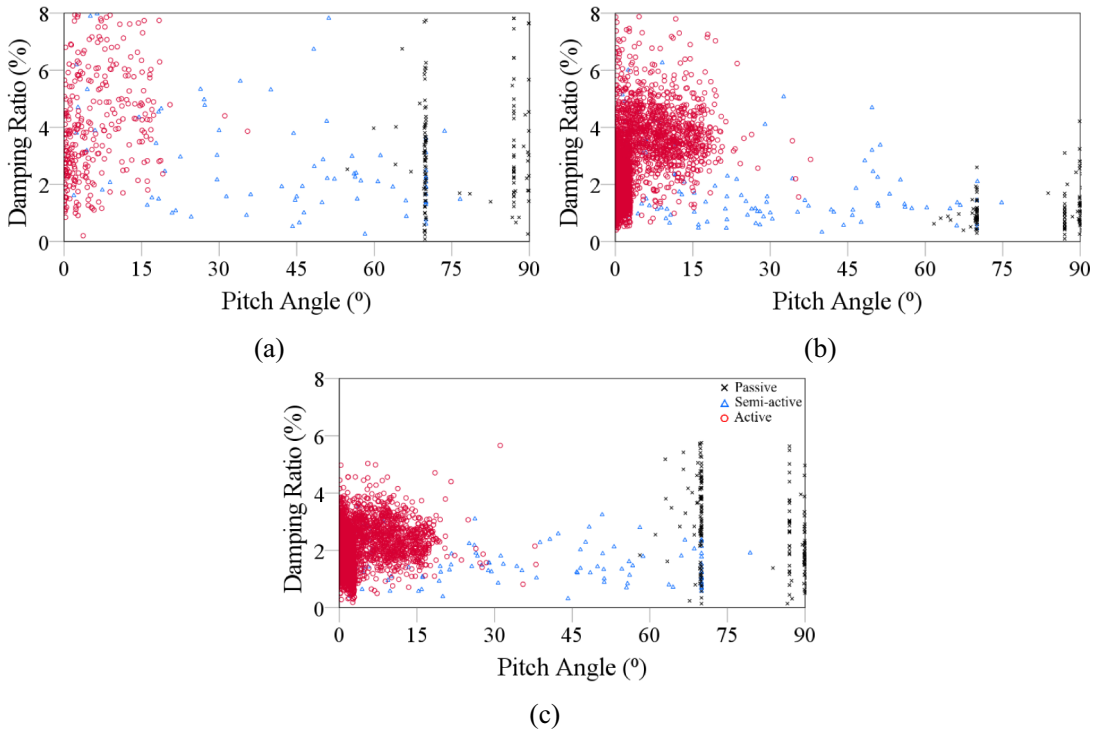

Fig. 20 Relationships between pitch angle and damping estimates for the frequency estimates at **a** 0.35 Hz, **b** 3.00 Hz, and **c** 8.29 Hz

1. All identified mode shapes are normalized by dividing their amplitudes at each level by the maximum amplitude of the corresponding mode shape.
2. The level (height) corresponding to the absolute maximum value in the vector form of an estimated mode is designated as the reference level.
3. A percentage value is calculated by counting the frequency of the designated reference level occurring at a particular level (Table 6).
4. The principal mode shapes are determined by averaging only the estimated mode shapes with the highest occurrence percentages (Fig. 21) and excluding the remaining estimates.
5. Modal Assurance Criterion (MAC) values are computed between each estimated mode shape and their corresponding principal mode shapes.
6. Correlations between the MAC values calculated in step 5 and the operational and environmental conditions are analyzed.

The relationship between the MAC values and rotor speed is shown in Fig. 22.

Most MAC values for the mode shape estimates at frequencies 0.35 Hz, 3.00 Hz, and 8.29 Hz are high, surpassing 95%, 95%, and 80%, respectively. A decrease in MAC values at around 11 RPM and 16 RPM rotor speeds is a consistent observation across all modes, where the decreasing trend in MAC values becomes more pronounced for the frequency estimates at 8.29 Hz. For the mode at 8.29 Hz, the MAC values form a secondary cluster around 90% at the 11–13 RPM and 15–16 RPM rotor speed levels. This observation indicates that this particular mode shape experiences spatial changes at these rotor speeds highlighting the importance of developing a structural health monitoring system where the effects of operational and environmental factors can be identified to avoid false alarms.

Table 6 Occurrence percentages of the reference level

	Level-2	Level-3	Level-4	Level-5
0.35 Hz	0%	0%	1%	99%
3.00 Hz	0%	63%	37%	0%
8.29 Hz	5%	0%	95%	0%

The relationship between the MAC values and wind speed is shown in Fig. 23.

For all modes, it can be said that the mode shapes notably differ from the principal mode shapes at wind speeds between 1–4 m/s which is the range where the switching between the passive or semi-active states occurs. Calculated MAC values drop around the wind speed ranges of 4–8 m/s and 10–16 m/s for mode estimated at 8.29 Hz modal frequency. These two wind speed ranges correspond to the rotor angular speeds of 11–13 RPM and 15–16 RPM (Fig. 22c), respectively, where it should also be noted that they align with the second cluster observed for the frequency estimates at 8.29 Hz.

The relationship between the MAC values and pitch angle is shown in Fig. 24.

The standard deviation of the MAC values decreases as the pitch angle of the blades increases. A reduction in the scattering of the MAC values is observed at pitch angles of 10°, 15°, and 15° for the mode shapes at 0.35 Hz, 3.00 Hz, and 8.29 Hz respectively. Consequently, the smaller MAC values at around 16 RPM rotor angular speed start to increase again as wind speed increases, while the pitch angles also increase. Eventually, the mode shape estimates start resembling the principal mode shapes more and more, indicated by larger MAC estimates.

The relationship between the MAC values and nacelle direction is shown in Fig. 25.

The nacelle direction clearly affects the turbine's mode shapes for the mode at 8.29 Hz. Lower MAC values are observed, particularly for the nacelle directions at around 30°, 150°, and 330° for the frequency estimate at 8.29 Hz.

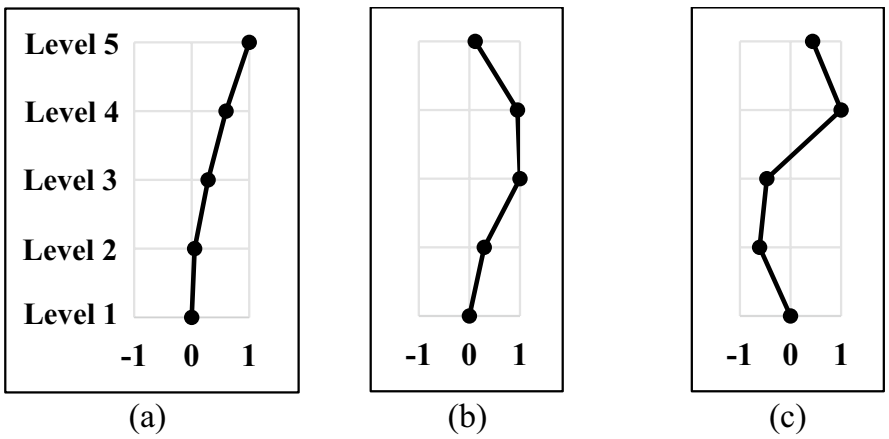

Fig. 21 The principal mode shapes for the frequency estimates at **a** 0.35 Hz, **b** 3.00 Hz, and **c** 8.29 Hz

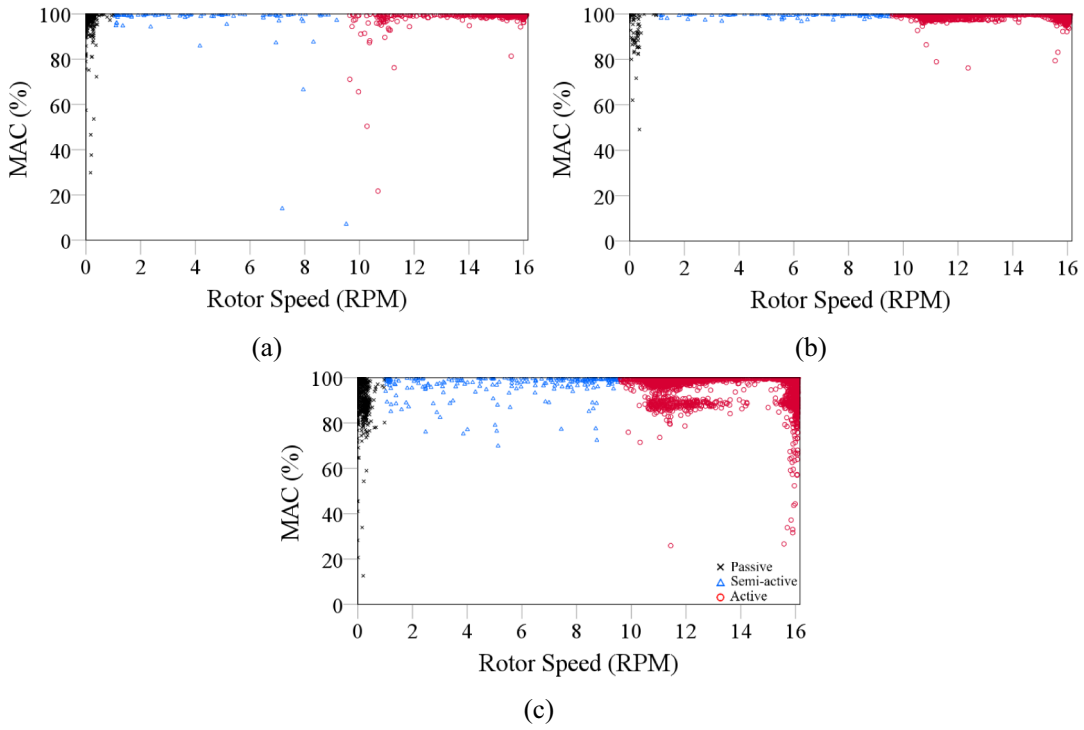

Fig. 22 Relationships between the rotor speed and MAC values for the frequency estimates at **a** 0.35 Hz, **b** 3.00 Hz, and **c** 8.29 Hz

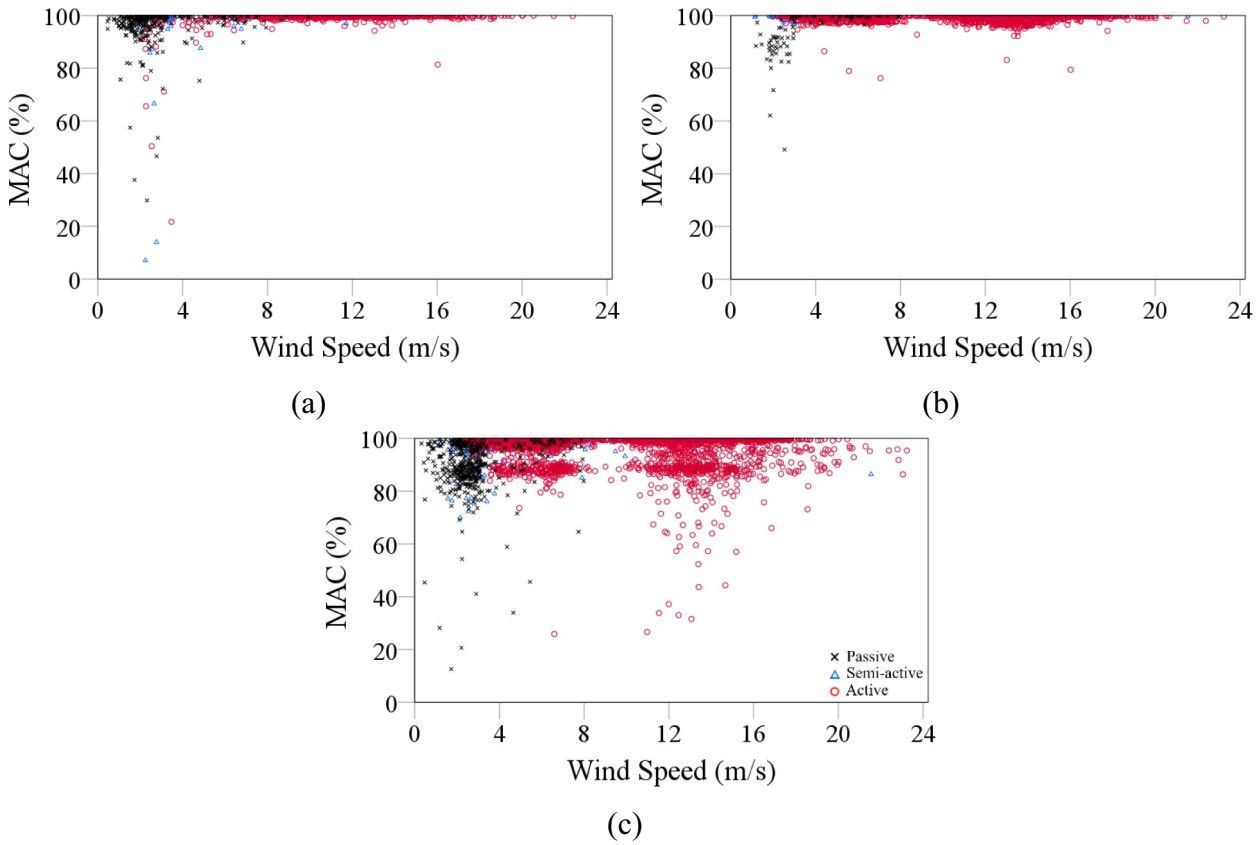

Fig. 23 Relationships between wind speed and the MAC values for the frequency estimates at **a** 0.35 Hz, **b** 3.00 Hz, and **c** 8.29 Hz

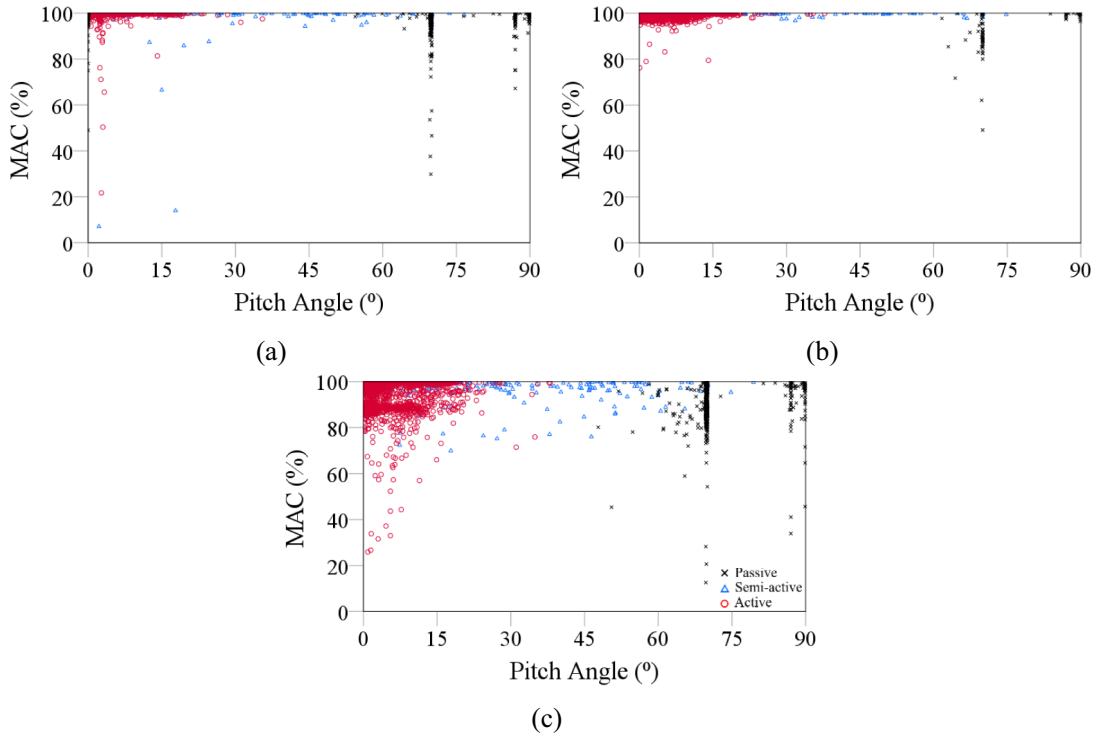

Fig. 24 Relationships between pitch angle and the MAC values for the frequency estimates at **a** 0.35 Hz, **b** 3.00 Hz, and **c** 8.29 Hz

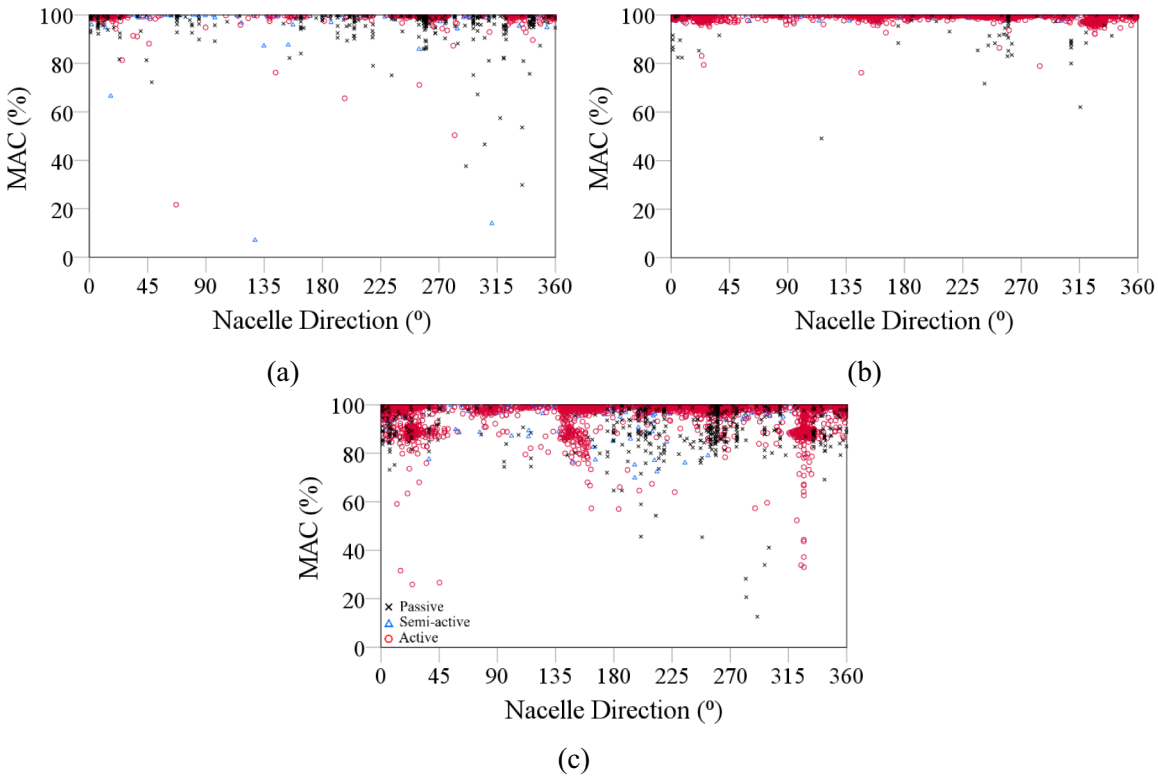

Fig. 25 Relationships between the nacelle direction and MAC values for the frequency estimates at **a** 0.35 Hz, **b** 3.00 Hz, and **c** 8.29 Hz

No clear relationship is observed between the mode shapes, temperature, relative humidity, and wind direction.

Conclusion

This paper mainly focuses on three key aspects of monitoring an operational wind turbine: (1) The design of a distributed data acquisition system tailored for an in-service wind turbine, (2) the development of a novel Autonomous and Continuous System Identification (ACSI) system, and (3) investigation of the effects of operational and environmental conditions on the estimated modal parameters (i.e., frequency, damping, and mode shapes) of the wind turbine tower.

The correlation analyses reveal important results for understanding how the operational and environmental conditions interact with the estimated modal parameters. For the mode at 3.00 Hz, modal frequency estimations corelate positively with rotor speed, attributed to the gyroscopic effect. Furthermore, after the rated wind speed of the turbine pitch angle of rotor blades is increased by turbine's control system to stabilize rotor speed as 16 RPM. This change in pitch angles, resulting in reduced wind loads on the rotor, leads to a decrease in frequency estimations for the mode estimated at 3.00 Hz. On the other hand, there is a negative correlation between the estimated modal frequencies and the ambient temperature. In a similar trend, the estimated damping ratios increase with increasing rotor speed, mainly due to the contribution of aerodynamic damping. The estimated mode shapes of the wind turbine are affected mainly by the nacelle direction and the rotor speed.

Additionally, the change in pitch angles significantly reduces scattering in all of the estimated modal parameters, which can be attributed to the fact that under faster rotor speeds, better excitation conditions occur. The Autonomous and Continuous System Identification (ACSI) system will continue to acquire and process data from the wind turbine, enabling further research to be conducted and insights to be withdrawn regarding the dynamics of the turbine tower. In the future, a predictive digital twin model for the turbine can be developed using artificial intelligence tools where the model can be trained with the data acquired by the system presented here. The results obtained in this study clearly show that the operational and environmental factors must be considered to develop a structural health monitoring system for operational wind turbines. For the horizontal axis wind turbines, the correlations between the identified modal parameters and operational/environmental conditions presented in this study can be generalized.

Acknowledgements The authors would like to extend their gratitude to The Scientific and Technological Research Council of Turkey (TÜBİTAK) for the financial support under the contract number 120M218. They also wish to thank Dost Enerji for their technical support for the fieldwork conducted and Kentkart A.Ş. for providing equipment assistance. All the views, findings, conclusions, and recommendations expressed in this publication are those of the authors and do not necessarily reflect the opinions of the sponsoring organizations. The authors would like to thank Ozgur Egilmez, Cemalettin Donmez, Carmen Amaddeo, Yasar Taner, and Veysel Yurtseven for the support to carry out this research work.

Funding Open access funding provided by the Scientific and Technological Research Council of Türkiye (TÜBİTAK).

Declarations

Conflict of Interest On behalf of all authors, the corresponding author states that there is no conflict of interest.

References

1. World Wind Energy Association [WWEA] (2024). Wind Power Capacity in the Net Zero Scenario. https://www.iea.org/reports/wind-electricity. Accessed 3 Apr 2024
2. Hu WH, Thöns S, Rohrmann RG, Said S, Rücker W (2015) Vibration-based structural health monitoring of a wind turbine system. Part I: Resonance phenomenon Eng Struct 89:260–272. https://doi.org/10.1016/j.engstruct.2014.12.034
3. Hu WH, Thöns S, Rohrmann RG, Said S, Rücker W (2015) Vibration-based structural health monitoring of a wind turbine system Part II: Environmental/operational effects on dynamic properties. Eng Struct 89:273–290. https://doi.org/10.1016/j.engstruct.2014.12.035
4. Song M, Mehr NP, Moaveni B, Hines E, Ebrahimian H, Bajric A (2023) One year monitoring of an offshore wind turbine: Variability of modal parameters to ambient and operational conditions. Eng Struct 297:117022. https://doi.org/10.1016/j.engstruct.2023.117022
5. Tcherniak D, Chauhan S, Hansen MH (2010) Applicability limits of operational modal analysis to operational wind turbines. In: IMAC XXVIII: A Conf on Struct Dyn, Jacksonville, FL, USA.
6. Tcherniak D, Allen MS (2015) Experimental characterization of an operating Vestas V27 wind turbine using harmonic power spectra and OMA SSI. In: 6th Int Oper Modal Anal Conf, Gijon, Spain.
7. Guillaume P, Verboven P, Vanlanduit S, Van Der Auweraer H, Peeters B (2003) A poly-reference implementation of the least-squares complex frequency-domain estimator. In/; Proc of IMAC (21:183–192). Kissimmee, FL: A Conf & Expo on Struct Dyn, Society for Experimental Mechanics

8. Peeters B, Van der Auweraer H, Guillaume P, Leuridan J (2004) The PolyMAX frequency-domain method: a new standard for modal parameter estimation? Shock and Vib 11(3–4):395–409. https://doi.org/10.1155/2004/523692
9. El-Kafafy M, Guillaume P, Peeters B (2013) Modal parameter estimation by combining stochastic and deterministic frequency-domain approaches. Mech Sys and Signal Process 35(1–2):52–68. https://doi.org/10.1016/j.ymssp.2012.08.025
10. James III GH, Carne TG, Lauffer JP (1993) The natural excitation technique (NExT) for modal parameter extraction from operating wind turbines (No. SAND-92–1666). Sandia National Labs., Albuquerque, NM (United States).
11. Häckell MW, Rolfes R (2013) Monitoring a 5 MW offshore wind energy converter—Condition parameters and triangulation based extraction of modal parameters. Mech Syst Signal Process 40(1):322–343. https://doi.org/10.1016/j.ymssp.2013.04.004
12. Kilic G, Unluturk MS (2015) Testing of wind turbine towers using wireless sensor network and accelerometer. Renew Energy 75:318–325. https://doi.org/10.1016/j.renene.2014.10.010
13. Alves MM, Pirmez L, Rossetto S, Delicato FC et al (2017) Damage prediction for wind turbines using wireless sensor and actuator networks. J of Netw and Compu App 80:123–140. https://doi.org/10.1016/j.jnca.2016.12.027
14. Avendaño-Valencia LD, Fassois SD (2017) Damage/fault diagnosis in an operating wind turbine under uncertainty via a vibration response Gaussian mixture random coefficient model based framework. Mech Sys and Signal Process 91:326–353. https://doi.org/10.1016/j.ymssp.2016.11.028
15. García D, Tcherniak D (2019) An experimental study on the data-driven structural health monitoring of large wind turbine blades using a single accelerometer and actuator. Mech Sys and Signal Process 127:102–119. https://doi.org/10.1016/j.ymssp.2019.02.062
16. Kim HC, Kim MH, Choe DE (2019) Structural health monitoring of towers and blades for floating offshore wind turbines using operational modal analysis and modal properties with numerical-sensor signals. Ocean Eng 188:106226. https://doi.org/10.1016/j.oceaneng.2019.106226
17. Zhou L, Li Y, Liu F, Jiang Z, Yu Q, Liu L (2019) Investigation of dynamic characteristics of a monopile wind turbine based on sea test. Ocean Eng 189:106308. https://doi.org/10.1016/j.oceaneng.2019.106308
18. Zhao X, Lang Z (2019) Baseline model based structural health monitoring method under varying environment. Renew Energy 138:1166–1175. https://doi.org/10.1016/j.renene.2019.02.007
19. Chen C, Duffour P, Fromme P (2020) Modelling wind turbine tower-rotor interaction through an aerodynamic damping matrix. J Sound Vib 489:115667. https://doi.org/10.1016/j.jsv.2020.115667
20. Pereira S, Pacheco J, Pimenta F, Moutinho C, Cunha Á, Magalhães F (2023) Contributions for enhanced tracking of (onshore) wind turbines modal parameters. Eng Struct 274:115120. https://doi.org/10.1016/j.engstruct.2022.115120
21. Dost Enerji (2024) Kores Kocadağ Wind Power Plant. https://www.dostenerji.com/en/plants/kores-kocadag-wpp/. Accessed 3 Apr 2024
22. Deniz A, Korkmaz KA, Irfanoglu A (2010) Probabilistic seismic hazard assessment for İzmir, Turkey. Pure and applied geophys 167:1475–1484. https://doi.org/10.1007/s00024-010-0129-6
23. Ali A, De Risi R, Sextos A (2021) Seismic assessment of wind turbines: How crucial is rotor-nacelle-assembly numerical modeling? Soil Dyn Earthq Eng 141:106483. https://doi.org/10.1016/j.soildyn.2020.106483
24. Chen B, Zhang Z, Hua X, Basu B, Nielsen SR (2017) Identification of aerodynamic damping in wind turbines using time-frequency analysis. Mech Syst Signal Process 91:198–214. https://doi.org/10.1016/j.ymssp.2017.01.010
25. Jiang J, Lian J, Dong X, Zhou H (2023) Research on the along-wind aerodynamic damping and its effect on vibration control of offshore wind turbine. Ocean Eng 274:113993. https://doi.org/10.1016/j.oceaneng.2023.113993
26. Yang C, Chen P, Cheng Z, Xiao L, Chen J, Liu L (2023) Aerodynamic damping of a semi-submersible floating wind turbine: An analytical, numerical and experimental study. Ocean Eng 281:114826. https://doi.org/10.1016/j.oceaneng.2023.114826